AD_____

Award Number: W81XWH-11-1-0279

TITLE: Receptor for Advanced Glycation End Products (RAGE) as a Novel Target for Inhibiting Breast Cancer Bone Metastasis

PRINCIPAL INVESTIGATOR: Ramesh K. Ganju

CONTRACTING ORGANIZATION: The Ohio State University
Columbus, OH 43210

REPORT DATE: April 2013

TYPE OF REPORT: Final

PREPARED FOR: U.S. Army Medical Research and Materiel Command
Fort Detrick, Maryland 21702-5012

# REPORT DOCUMENTATION PAGE

*Form Approved*
*OMB No. 0704-0188*



| 1. REPORT DATE *(DD-MM-YYYY)* | 2. REPORT TYPE | 3. DATES COVERED *(From - To)* |
|---|---|---|
| April 2013 | Final | 1 April 2011 - 31 March 2013 |

**4. TITLE AND SUBTITLE**
Receptor for Advanced Glycation End Products (RAGE) as a Novel Target for Inhibiting Breast Cancer Bone Metastasis

**5a. CONTRACT NUMBER**

**5b. GRANT NUMBER**
W81XWH-11-1-0279

**5c. PROGRAM ELEMENT NUMBER**

**6. AUTHOR(S)**
Ramesh Ganju

E-Mail: Ramesh.Ganju@osumc.edu

**5d. PROJECT NUMBER**

**5e. TASK NUMBER**

**5f. WORK UNIT NUMBER**

**7. PERFORMING ORGANIZATION NAME(S) AND ADDRESS(ES)**
The Ohio State University
Columbus, OH 43210

**8. PERFORMING ORGANIZATION REPORT NUMBER**

**9. SPONSORING / MONITORING AGENCY NAME(S) AND ADDRESS(ES)**
U.S. Army Medical Research and Materiel Command
Fort Detrick, Maryland 21702-5012

**10. SPONSOR/MONITOR'S ACRONYM(S)**

**11. SPONSOR/MONITOR'S REPORT NUMBER(S)**

**12. DISTRIBUTION / AVAILABILITY STATEMENT**
Approved for Public Release; Distribution Unlimited

**13. SUPPLEMENTARY NOTES**

**14. ABSTRACT**

Receptor for advanced glycation end products (RAGE) has been shown to play an important role in inflammation and cancer. However, not much is known about its role in breast cancer progression and metastasis, especially to bone. We have shown that RAGE may play an important role in osteoclast formations, which are known to mediate osteolytic lesions at the site of bone metastatic tumors. Furthermore, we have shown that RAGE may regulate breast tumor progression using RAGE knockout mice. We have shown that mS100a7a15/RAGE axis regulates in vivo tumor growth using mS100a7a15 transgenic mouse models. RAGE may enhance tumor growth and metastasis by modulating recruitment of M2 macrophages to the tumor microenvironment. We also have shown that RAGE is highly expressed in breast cancer cells that metastasize to bone and RAGE regulates chemotaxis and wound healing of triple negative breast cancer cells.

**15. SUBJECT TERMS**
RAGE, breast cancer, S100A7, tumor growth, metastasis

| 16. SECURITY CLASSIFICATION OF: | | | 17. LIMITATION OF ABSTRACT | 18. NUMBER OF PAGES | 19a. NAME OF RESPONSIBLE PERSON |
|---|---|---|---|---|---|
| a. REPORT | b. ABSTRACT | c. THIS PAGE | | | USAMRMC |
| U | U | U | UU | 46 | 19b. TELEPHONE NUMBER *(include area code)* |

## Table of Contents

1. **INTRODUCTION:** Receptor for advanced glycation end products (RAGE) expression has been shown to be detected in human cancers, including 63% of breast carcinomas. RAGE has been shown to play an important role in inflammation and cancer. RAGE also regulates trafficking of myeloid-derived suppressor cells, which have been shown to suppress anti-tumorigenic responses. Furthermore, RAGE has also been shown to play an important role in insulin resistance and diabetes, which is linked to breast cancer progression and metastasis. Our hypothesis is that targeting RAGE plays an important role in breast cancer metastasis, especially to bone. S100A7, which plays an important role in breast cancer progression and metastasis, was recently shown to bind to RAGE. We analyzed S100A7/RAGE-mediated effects on osteoclast formation. We also analyzed the role of RAGE on tumor growth using RAGE knockout mouse models, as well as in mS100a7a15 (murine ortholog of human S100A7) transgenic mouse models. We also analyzed the role of RAGE in regulating breast cancer chemotaxis, chemoinvasion, and wound healing *in vitro*.

2. **KEYWORDS:** RAGE, breast cancer, S100A7, tumor growth, metastasis

**3. OVERALL PROJECT SUMMARY:** We observed high expression of RAGE in ~50-60% of breast invasive ductal carcinomas compared to benign mammary epithelium. RAGE expression was analyzed in tissue microarray containing 120 breast cancer patient samples by immunohistochemical analysis using antibody against RAGE (Abcam) (Fig. 1). Previously, constructed paraffin-embedded, formalin-fixed 120 cases of breast carcinoma tissue microarray slides were obtained from the archives of the Ohio State University Department of Pathology. Antigen retrieval on TMA slides was performed by Heat-Induced Epitope Retrieval (HIER,) where slides were placed in Dako TRS solution (pH 6.1) for 25 minutes at 94°C and cooled for 15 minutes. Slides were then placed on a Dako Autostainer, immunostaining system, for use with immunohistochemistry. Slides were incubated for 60 minutes in primary RAGE antibodies (1:1400, Abcam) and detected using a labeled polymer system, ImmPRESS Anti-Rabbit Ig (peroxidase) Kit (Vector Laboratories, CA) as per manufacturer's protocol. Staining was visualized with DAB chromogen. Slides were then counterstained in Richard Allen hematoxylin, dehydrated through graded ethanol solutions and cover slipped. We also analyzed RAGE expression by flow cytometry using RAGE antibodies (Abcam) in different breast cancer cell lines and found that RAGE is highly expression in triple-negative breast cancer cell line (TNBC), SCP2, which has been shown to metastasize to bone (Table 1). Briefly, cells ($1x10^6$) were incubated with anti-RAGE (1:100) in a total volume of 400 µl of HEPES-buffered Hanks' balanced salt solution for 60 min at 4 °C. The cells were then washed and incubated with fluorescein isothiocyanate-conjugated (FITC)-anti-rabbit IgG for 60 min at 4 °C. The cells were washed again and analyzed for cell-surface expression of the receptor on a BD Biosciences FACScan cytometer. Next, we analyzed the role of RAGE in modulating breast cancer chemotaxis, chemoinvasion, and wound healing parameters that determine the metastatic potential of cells. We have shown that RAGE is expressed on monocytic cell line THP1 by flow cytometry using RAGE antibodies (Fig. 2A) and breast cancer cell line MDA-MB-231. **Cells** were incubated in serum free media for 48h and after the treatment period, the supernatants were collected, concentrated and subjected to Western blot analysis. (A, lower) THP1 cells were incubated with phorbol myristic acid (PMA, 100ng/ml) for 48 h to differentiate into macrophages. These differentiated macrophages or MDA-MB-231 cells ($1x10^6$) were incubated with anti-RAGE (1:100) in a total volume of 400 µl of HEPES-buffered Hanks' balanced salt solution for 60 min at 4 °C. The cells were then washed and incubated with fluorescein isothiocyanate-conjugated (FITC)-anti-rabbit IgG for 60 min at 4 °C. The cells were washed again and analyzed for cell-surface expression of the receptor on a BD Biosciences FACScan cytometer. Moreover overexpression of S100A7 in MDA-MB-231 (TNBC) cells significantly increased the intracellular as well as surface expression of RAGE (Fig. 2A). We also showed that recombinant S100A7 enhances migration of THP1 (Fig. 2B) and MDA-MB-231 (Fig. 2C) and wound healing of MDA-MB-231 (Fig. 2D) and the effects were mediated through RAGE, as pretreatment of RAGE neutralizing antibody inhibited S100A7-induced migration and wound healing in these cells **as described** (Fig. 2B-D). THP1-differentiated macrophages were pre-treated with RAGE neutralizing antibody 10µg or IgG control for 30 minutes. These treated cells were subjected to a chemotaxis assay towards conditioned media (CM) of S100A7 overexpressing MDA-MB-231 or vector cells using transwell plates. To further explore the mechanisms associated with these functional effects, we found that S100A7 significantly increased the phosphorylation of STAT3 (p-STAT3), p-AKT and ERK1/2 in MDA-MB-231 and SCP2 cells and the effects were mediated through RAGE, as pretreatment of Soluble RAGE (S-RAGE) reduced S100A7-induced activation of STAT3 and ERK1/2 in SCP2 cells (Fig. 3). Furthermore, we observed that

RAGE overexpression enhances epidermal growth factor (EGF)/insulin growth factor (IGF)-induced migration in MCF7 breast cancer cell line (Fig. 4). Overall, these studies suggest that RAGE modulates chemoinvasion and signaling in breast cancer cell lines.

Bone metastasis is associated with increased morbidity in breast cancer patients. The most common manifestation of bone metastasis is osteolysis which is associated with osteoclast formation. We also showed that RAGE is expressed by RAW264.7 cells, which are precursors for osteoclasts (Fig. 5). Briefly, cells ($1x10^6$) were incubated with anti-RAGE (1:100) in a total volume of 400 µl of HEPES-buffered Hanks' balanced salt solution for 60 min at 4 °C. The cells were then washed and incubated with fluorescein isothiocyanate-conjugated (FITC)-anti-rabbit IgG for 60 min at 4 °C. The cells were washed again and analyzed for cell-surface expression of the receptor on a BD Biosciences FACScan cytometer. In addition, RAGE regulates chemotaxis of these cells (Fig. 6). S100A7 has been shown to be the functional ligand for RAGE. We also observed that mS100a7a15 (mouse homologue of human S100A7) enhances chemotaxis of RAW264.7 cells *in vitro* and RAGE neutralizing antibodies inhibited the mS100a7a15 enhance chemotaxis of RAW264.7 cells compared to IgG control (Fig. 6). Murine macrophage RAW264.7 cells were pretreated 1hour with RAGE blocking antibody or control IgG (20 µg) and $1x10^5$ cells were plated on the top chamber of 8 µm pore polycarbonate membrane filters and medium in absence or presence of murine mS100a7a15 (100ng/mL) was placed in the lower chamber. After 12 hours of incubation, cells that migrated across the filter towards medium with or without murine mS100a7a15 (100ng/mL) were fixed, stained and counted by bright-field microscopy in five random fields. Moreover, mS100a7a15 enhances STAT3 activation in RAW264.7 cells and blocking of RAGE by neutralizing antibodies reduced the activation of STAT3 as described (Fig. 6). MDA-MB231 cells were treated for 1 hour with RAGE blocking antibody or control IgG (20 µg) and stimulated with 100 ng/ml of recS100a7a15 for different time periods. Cell lysates were analyzed for Phospho-ERK (p-ERK), ERK and p-STAT3 by Immunoblotting. We found mS100a7a15-increased osteoclast formation in RAW264.7 cells. Osteoclast-like cells were scored by counting the number of TRAP-positive cells containing three or more nuclei. Next, to confirm the role of RAGE in osteoclast formation, we did the experiments in presence of RAGE neutralizing antibody or control IgG. We found the RAGE neutralizing antibodies significantly reduced the number of TRAP-positive cells compared to IgG control (Fig. 7). RAW 264.7 cells were incubated with or without mS100a7a15 100 ng/mL in the presence of RAGE blocking antibody or control IgG (20 µg) for 7 days and TRAP activity was measured as a marker of osteoclastic differentiation. RAW 264.7 cells grown on 6-well plate were fixed with 10% (v/v) formalin and washed with PBS. They were then incubated with solution of (p-nitrophenyl, and Tartarate) at 37°C for 30 min. After the incubation, the solution was removed from each well and Washed with distilled water and counter staining for 2 minutes in Hematoxylin. The purplish to dark brown granules, indicate the formation of TRAP. Furthermore, the osteoclasts were determined by Real time PCR using gene specific primers against cathepsin K (Cstk). It has been shown that osteoclasts express many proteases including cathepsins and matrix metalloproteases (MMPs) and CstK is the major bone-degrading enzyme. We found mS100a7a15-increased Cstk mRNA levels in RAW264.7 cells and RAGE neutralizing antibodies reduced the levels of Cstk mRNA levels (Fig. 7). The numbers of TRAP positive cells were determined by real time PCR using gene specific primers against cathepsin K. Overall, these studies suggest that RAGE regulates osteoclast formation *in vitro.*

We analyzed the role of RAGE expressed on host cells on breast cancer growth using RAGE knockout mouse models. PyMT cells ($1x10^5$) derived from MMTV-PyMT mice, were orthotopically injected into the #4 MG of the RAGE KO and wildtype C57BL/6 mice (n=5). (A) Tumor volume was measured every week in these mice was assessed periodically and calculated using the formula length x (width)2/2. We observed reduced growth of PyMT cells injected orthotopically into the mammary glands of RAGE knockout mice compared to wild-type mice (Fig. 8A-C). Similarly, IHC staining from tumor tissue obtained from RAGE KO displayed reduced expression of Ki67 (proliferation marker), CD31 (angiogenic marker) and F4/80, (macrophage recruitment) compared to wild type mice (Fig. 8D). Briefly, antigen retrieval on RAGE knockout and wildtype tumor tissue slides were performed by Heat-Induced Epitope Retrieval (HIER,) where slides were placed in Dako TRS solution (pH 6.1) for 25 minutes at 94°C and cooled for 15 minutes. Slides were then placed on a Dako Autostainer, immunostaining system, for use with immunohistochemistry. Slides were incubated for 60 minutes in primary CD31 (Santa Cruz 1:100) or F4/80 (AbD Serotec, 1:50) or Ki67 (Neomarkers, 1:100) RAGE antibodies (1:1400, Abcam) and detected using a

labeled polymer system, ImmPRESS Anti-Rabbit Ig (peroxidase) Kit (Vector Laboratories, CA) as per manufacturer's protocol. Vectastain Elite ABC reagents (Vector Laboratories) using avidin DH:biotinylated horseradish peroxidase H complex with 3,3′-diaminobenzidine (Polysciences) and Mayer's hematoxylin (Fisher Scientific) were used for detection of the bound antibodies. This data suggests that RAGE plays an important role in breast cancer growth by modulating macrophage recruitment. Currently, we are analyzing the role of RAGE in breast cancer metastasis to bone using this model system.

We also showed that RAGE is expressed by MVT-1 cells. MVT1 cells ($1x10^6$) were incubated with anti-RAGE (1:100) in a total volume of 400 µl of HEPES-buffered Hanks' balanced salt solution for 60 min at 4 °C. The cells were then washed and incubated with fluorescein isothiocyanate-conjugated (FITC)-anti-rabbit IgG for 60 min at 4 °C. The cells were washed again and analyzed for cell-surface expression of the receptor on a BD Biosciences FACScan cytometer (Fig. 9A) MVT1 cells are highly aggressive cell lines and murine ortholog of human S100A7 (mS100a7a15) significantly increased the phosphorylation of ERK in MVT-1 this cell line (Fig. 9C). MVT-1 cells were stimulated with 100 ng/ml of recmS100a7a15 at different time points as shown in Fig. 9C and cell lysates were analyzed for p-ERK expression by Western Blot.

We further analyzed the role of mS100a7a15/RAGE in tumor progression by implanting highly aggressive MVT-1 cells into the mammary gland of MMTV-mS100a7a15 mice. MVT-1 cells ($1x10^5$) cells were injected into the mammary gland (#4) of the MMTV-mS100a7a15 mice (n =5). Five days prior to injection, mice (n=5) were fed with 1 g/kg Dox-chow to induce mS100a7a15 and mice maintained on normal diet served as control. When tumor becomes palpable, mice will be injected mice with 80 µg/kg body weight of RAGE neutralizing or IgG control antibodies every alternate day for 4 weeks. Tumor volume and growth measured every week in these mice was assessed periodically and calculated using the formula length x (width)2/2 (Fig. 10). Interestingly, MVT-1–derived tumor growth was enhanced in doxycycline-treated MMTV-mS100a7a15 mice compared with the un-induced mice (Fig. 10). The RAGE neutralizing antibodies significantly reduced the MVT-1–derived tumor growth in doxycycline-treated MMTV-mS100a7a15 mice compared with control mice (Fig. 10). Tumor associated macrophages (TAMs) have been shown to be a major component of inflammatory infiltrates seen in tumors. We analyzed M2 macrophage infiltration in the tumors by flow cytometry. Briefly, tumor cells of MVT1-derived tumors from doxycycline-treated or untreated MMTV-mS100a7a15 mice were subjected to flow cytometry for macrophage marker CD11b/F4/80. Briefly, tumor cells ($1x10^6$) were incubated with anti-F4/80 PE and anti-Cd11b APC (1:100) in a total volume of 400 µl of HEPES-buffered Hanks' balanced salt solution for 60 min at 4 °C. The cells were washed again and analyzed for cell-surface expression of the receptor on a BD Biosciences FACScan cytometer. As shown in Fig. 10, the CD11b, F4/80 macrophage infiltration was increased in doxycycline-induced MMTV-mS100a7a15 compared with uninduced mice and RAGE neutralization significantly reduced M2 macrophage recruitment in tumors of doxycycline-induced MMTV-mS100a7a15 expressing mice (Fig. 10).

## 4. KEY RESEARCH ACCOMPLISHMENTS

- RAGE is expressed in human breast invasive ductal carcinomas.
- Breast cancer cell lines that metastasize to bone express a higher amount of RAGE.
- RAGE regulates chemotaxis of preosteoclasts mediated by S100A7/mS100a7a15.
- mS100a7a15/RAGE axis regulates osteoclast formation *in vitro*.
- RAGE knockout mice showed significantly reduced breast tumor growth.
- RAGE regulates tumor growth by modulating recruitment of M2 macrophages to the tumor microenvironment and thereby might be responsible for metastasis.

- Mouse breast cancer cell lines show reduced growth in mS100a7a15 transgenic mice treated with RAGE neutralizing antibody compared to control.

- S100A7/RAGE axis activates STAT3 and ERK1/2.

- Blocking of S100A7/RAGE axis by soluble RAGE or neutralizing antibodies could reduce RAGE-mediated functional effects.

- RAGE neutralizing antibody inhibits chemotaxis/chemoinvasion and wound healing of breast cancer cells.

**5. CONCLUSION:** We have shown that RAGE is expressed in human breast cancer patient samples. We have also shown that RAGE is the receptor for S100A7. Furthermore, we have shown that breast cancer cell lines that metastasize to bone express higher amounts of RAGE. We also showed that RAGE neutralizing antibodies significantly reduced the number of S100A7-induced osteoclast formation compared to IgG control. In addition, we have shown that the mouse ortholog of S100A7 (mS100a7a15) upon binding to RAGE may regulate osteoclast formation *in vitro*. RAGE mediates its functional effects by activating STAT3 and ERK1/2. Using RAGE neutralizing antibodies, we have shown that RAGE regulates chemoinvasion/wound healing of breast cancer cells. Our data also suggests that RAGE present in the host cells regulate tumor growth, as reduced tumor growth was obtained in RAGE knockout mouse models compared to wild-type and the blocking of RAGE by neutralizing antibodies reduced tumor growth in vivo. Our studies also indicate that RAGE regulates tumor growth by modulating recruitment of M2 macrophages to the tumor microenvironment. Recruitment of TAMs into tumor microenvironment may in turn stimulate tumor growth and metastasis by enhancing expression of pro metastatic and proinflammatory molecules. Thus, these studies suggest that S100A7 through RAGE may enhance tumor growth and metastasis.

**6. PUBLICATIONS, ABSTRACTS, AND PRESENTATIONS:**

a. List all manuscripts submitted for publication during the period covered by this report resulting from this project. Include those in the categories of lay press, peer-reviewed scientific journals, invited articles, and abstracts. Each entry shall include the author(s), article title, journal name, book title, editors(s), publisher, volume number, page number(s), date, DOI, PMID, and/or ISBN.

**(1)** Lay Press: Nothing to report.
**(2)** Peer-Reviewed Scientific Journals:

Nasser MW**,** Qamri Z, Deol YS, Ravi J, Powell CA, Trikha P, Shilo K, Leone G, Bai X-F, Zou X, Wolf R, Yuspa S, Ganju RK**.** S100A7 enhances mammary tumorigenesis through upregulation of inflammatory pathways. Cancer Res**.** 2012. **72**(3):604-15.

Sneh A, Deol YS, Ganju A, Shilo K, Rosol TJ, Nasser MW, Ganju RK**.** Differential role of psoriasin (S100A7) in estrogen receptor α positive and negative breast cancer cells occur through actin remodeling. Breast Cancer Res Treat. 2013 Apr;138(3):727-39.

**(3)** Invited Articles: Nothing to report.
**(4)** Abstracts:

Gina Pietras Spohn, Mohd W. Nasser, Ramesh K. Ganju**.** Department of Pathology, The Ohio State University Medical Center, 2012 Trainee Research Day, April 18, 2012. Receptor for Advanced Glycation End Products (RAGE) as a Novel Target for Inhibiting Breast Cancer Metastasis. Poster Presentation.

b. List presentations made during the last year (international, national, local societies, military meetings, etc.). Use an asterisk (*) if presentation produced a manuscript.

**7. INVENTIONS, PATENTS AND LICENSES:** Nothing to report.

**8. REPORTABLE OUTCOMES:**

Nasser MW**,** Qamri Z, Deol YS, Ravi J, Powell CA, Trikha P, Shilo K, Leone G, Bai X-F, Zou X, Wolf R, Yuspa S, Ganju RK**.** S100A7 enhances mammary tumorigenesis through upregulation of inflammatory pathways. Cancer Res**.** 2012. **72**(3):604-15.

Sneh A, Deol YS, Ganju A, Shilo K, Rosol TJ, Nasser MW, Ganju RK**.** Differential role of psoriasin (S100A7) in estrogen receptor α positive and negative breast cancer cells occur through actin remodeling. Breast Cancer Res Treat. 2013 Apr;138(3):727-39.

Gina Pietras Spohn, Mohd W. Nasser, Ramesh K. Ganju**.** Department of Pathology, The Ohio State University Medical Center, 2012 Trainee Research Day, April 18, 2012. Receptor for Advanced Glycation End Products (RAGE) as a Novel Target for Inhibiting Breast Cancer Metastasis. Poster Presentation.

**9. OTHER ACHIEVEMENTS:** Nothing to report.

# Appendix 1

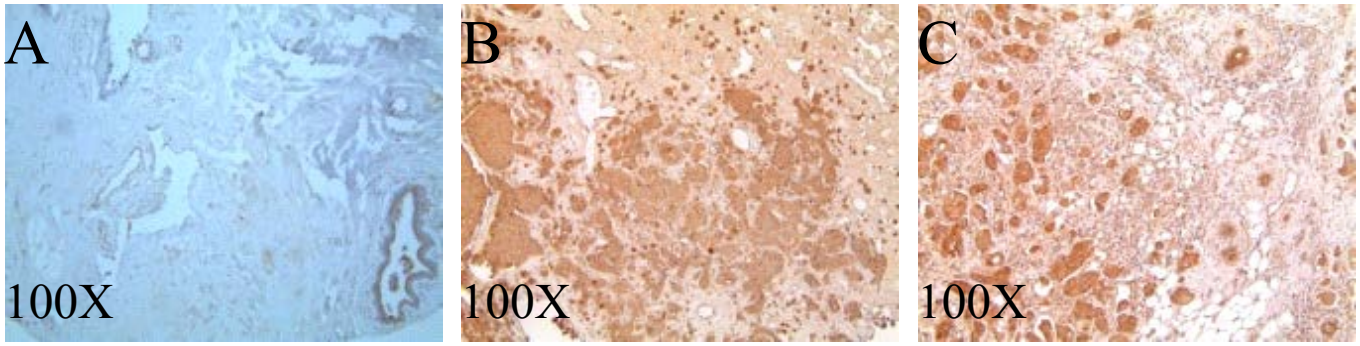


**Fig. 1. Expression of RAGE in breast cancer patient samples.** Paraffin-embedded, formalin-fixed specimens were analyzed for RAGE (B-C) by IHC. Normal breast tissue (A), Invasive ductal carcinoma (B & C). Previously constructed paraffin-embedded, formalin-fixed 120 cases of breast carcinoma tissue microarray slides were obtained from the archives of the Ohio State University Department of Pathology. Antigen retrieval onTMA slides was performed by Heat-Induced Epitope Retrieval (HIER,) where slides were placed in Dako TRS solution (pH 6.1) for 25 minutes at 94°C and cooled for 15 minutes. Slides were then placed on a Dako Autostainer, immunostaining system, for use with immunohistochemistry. Slides were incubated for 60 minutes in primary RAGE antibodies (1:1400, Abcam) and detected using a labeled polymer system, ImmPRESS Anti-Rabbit Ig (peroxidase) Kit (Vector Laboratories, CA) as per manufacturer's protocol. Staining was visualized with DAB chromogen. Slides were then counterstained in Richard Allen hematoxylin, dehydrated through graded ethanol solutions and cover slipped.

| Table 1. RAGE expression in ERα⁻ and ERα⁺ cells | | | |
|---|---|---|---|
| ERα⁻ | %RAGE | ERα⁺ | %RAGE |
| SCP2 | 71 | MCF7 | 2 |
| MB-231 | 57 | T47D | 8 |
| MB-453 | 56 | BT-474 | 11 |

Method: Cells (1x106) were incubated with anti-RAGE (1:100) in a total volume of 400 µl of HEPES-buffered Hanks' balanced salt solution for 60 min at 4 °C. The cells were then washed and incubated with fluorescein isothiocyanate-conjugated (FITC)-anti-rabbit IgG for 60 min at 4 °C. The cells were washed again and analyzed for cell-surface expression of the receptor on a BD Biosciences FACScan cytometer. The data were presented as % RAGE expression.

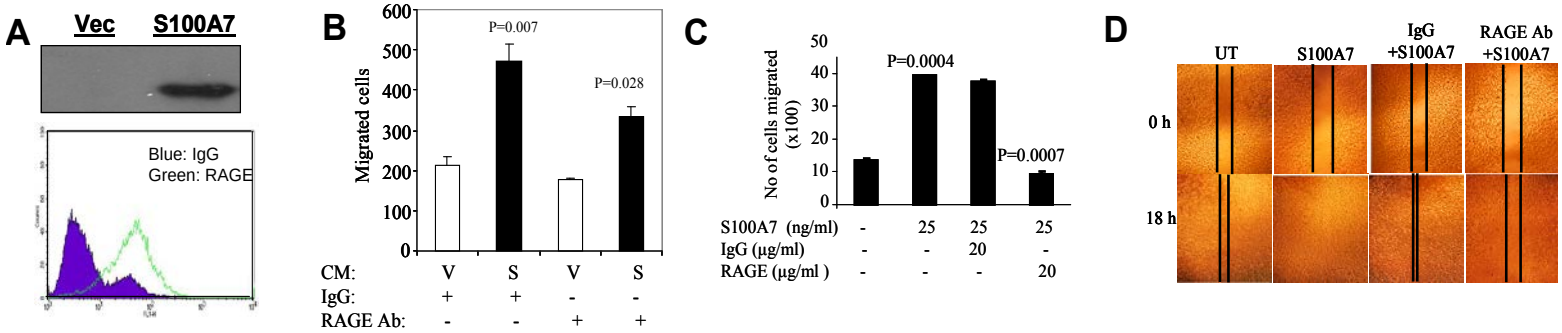


**Figure 2. RAGE mediates cell migration and wound healing in breast cancer cells and monocytes/macrophages.** (A, upper) Expression of soluble S100A7 expression in conditioned media of 231-Vector and 231-S100A7 cells by Western blot analysis. Cells were incubated in serum free media for 48h and after the treatment period, the supernatants were collected, concentrated and subjected to Western blot analysis. (A, lower) THP1 cells were incubated with phorbol myristic acid (PMA, 100ng/ml) for 48 h to differentiate into macrophages. These differentiated macrophages ($1x10^6$) were incubated with anti-RAGE (1:100) in a total volume of 400 µl of HEPES-buffered Hanks' balanced salt solution for 60 min at 4 °C. The cells were then washed and incubated with fluorescein isothiocyanate-conjugated (FITC)-anti-rabbit IgG for 60 min at 4 °C. The cells were washed again and analyzed for cell-surface expression of the receptor on a BD Biosciences FACScan cytometer. (B) These differentiated macrophages were subjected to a chemotaxis assay towards conditioned media (CM) of S100A7 overexpressing MDA-MB-231 or vector cells using transwell plates a. cell migration assay with CM containing S100A7 and control in cells pretreated with RAGE neutralizing or control IgG. (C) MDA-MB-231 cells were subjected to a chemotaxis assay towards recombinant purified human S100A7 (25 ng/ml) using transwell plates (BD) in presence of RAGE neutralizing antibody or control IgG. (D) MDA-MB-231 cells were stimulated with recS100A7 (25 ng/ml) for 18 h and subjected to wound scratch assay in presence of RAGE blocking antibody or control IgG under serum-free conditions.

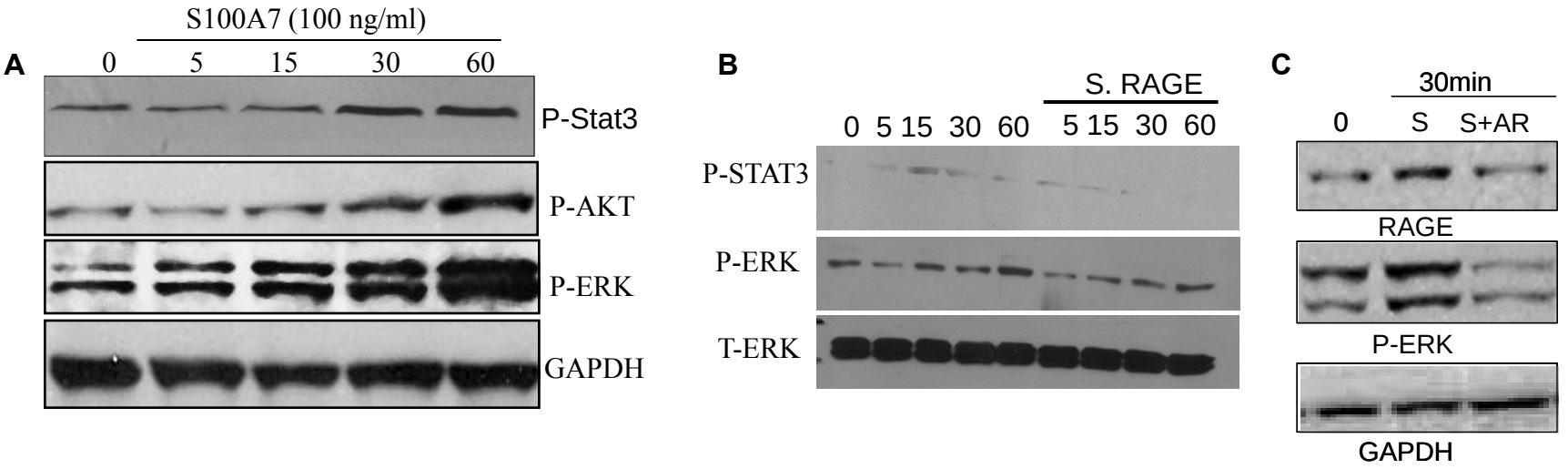


**Figure 3. RAGE induces signaling in breast cancer cells.** (A) MDA-MB231 breast cancer cells stimulated with 100 ng/ml of recS100A7 (S) and cell lysates were analyzed for p-ERK, p-AKT and p-STAT3 expression by WB. Blots were reprobed for GAPDH for loading controls. (B) SCP2 breast cancer cells stimulated with 100 ng/ml of recS100A7 (S) in presence or absence of soluble RAGE and cell lysates were analyzed for p-ERK and p-STAT3 expression by WB. (C) MDA-MB231 breast cancer cells stimulated with 100 ng/ml of recS100A7 (S) in presence or absence of RAGE neutralizing antibody (AR) and cell lysates were analyzed for p-ERK expression by WB. Blots were reprobed for GAPDH for loading controls.

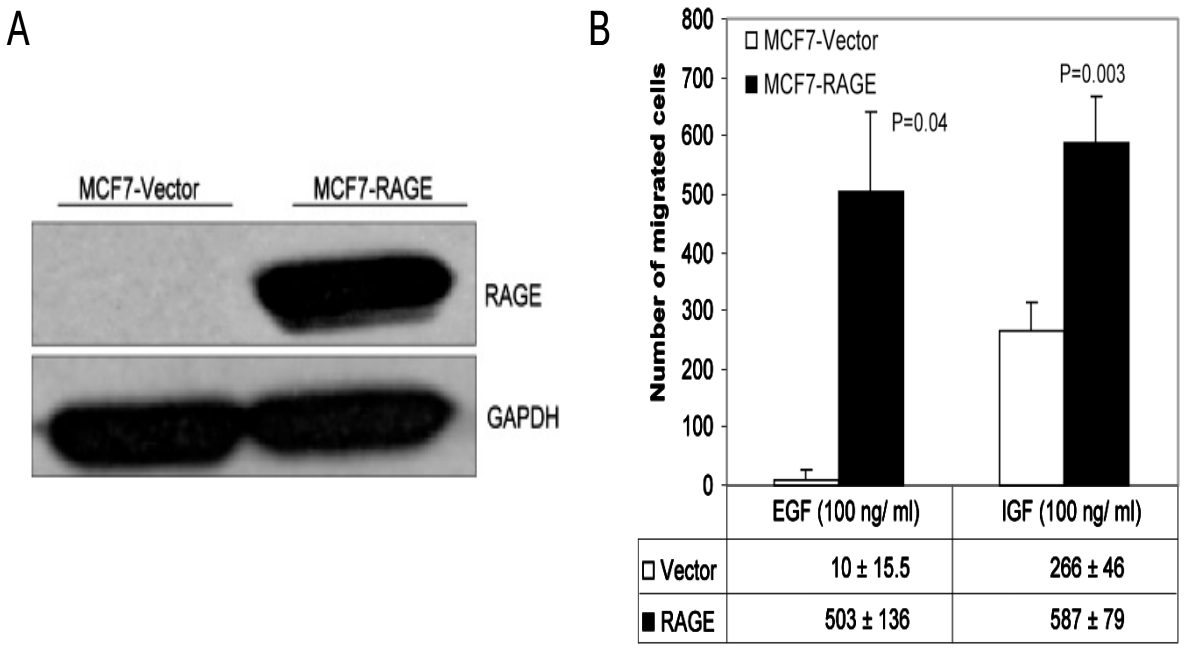


**Figure 4. RAGE overexpressing MCF-7 cells enhance EGF/IGF-induced migration.** (A). RAGE overexpression in MCF7 cells. MCF7 cells were transfected with pIRES2-EGFP (Invitrogen) or pIRES-2-EGFP-RAGE plasmids using Lipofectamine reagent according to the manufacturer's instructions and stable clones were generated using G418 (500µg/ml). (B). MCF7-Vector and MCF7-RAGE were subjected to a chemotaxis assay towards EGF (100ng/ml) and IGF (100ng/ml) using the 24-well Transwell plates. The lower surface of the insert was stained and cells were counted in an average of 5-highpower fields. Experiments were done in duplicate and repeated three times.

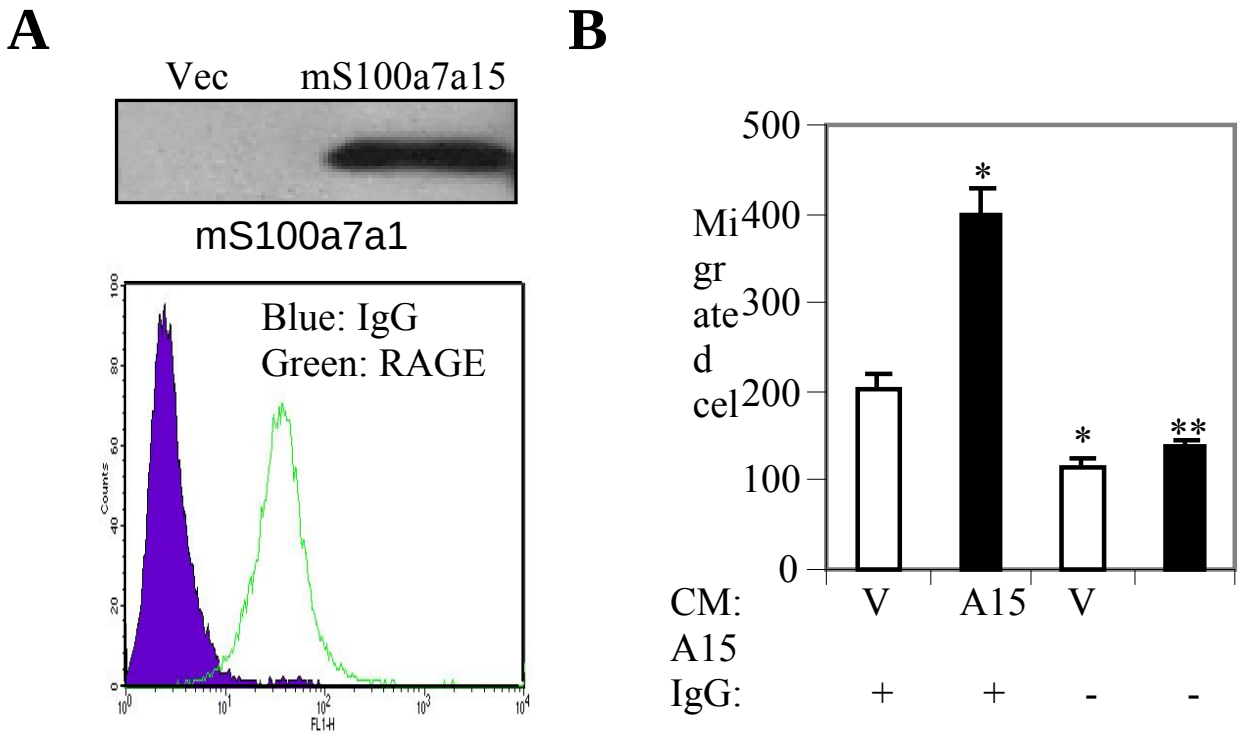


**Figure 5. Role of RAGE in chemotaxis of RAW264.7 cells.** (A, *upper*) WB of CM of Vec or mS100a7a15 overexpressing cells. (A, *lower*) FACS analysis of RAGE expression in RAW264.7 cells. Cells ($1x10^6$) were incubated with anti-RAGE (1:100) in a total volume of 400 µl of HEPES-buffered Hanks' balanced salt solution for 60 min at 4 °C. The cells were then washed and incubated with fluorescein isothiocyanate-conjugated (FITC)-anti-rabbit IgG for 60 min at 4 °C. The cells were washed again and analyzed for cell-surface expression of the receptor on a BD Biosciences FACScan cytometer. (B) Migration Assay. RAW264.7 cells were incubated with murine RAGE neutralizing or control IgG antibodies for 30 min and subjected to vector or mS100a7a15 CM-induced migration by seeding $0.5x10^6$ cells in the upper chamber of 8µm of transwell plates and CM of 231-vector or 231-mS100a7a15 cells in lower chamber and incubated overnight. The number of cells migrated were stained with Hema stain and counted in five different fields. V represents vector, S represents hS100A7 and A15 represents mS100a7a15. Graphs represent the mean ± SD for each experiment repeated three times with similar results.$^*$, $p<0.05$ and $^{**}$, $p<0.01$.

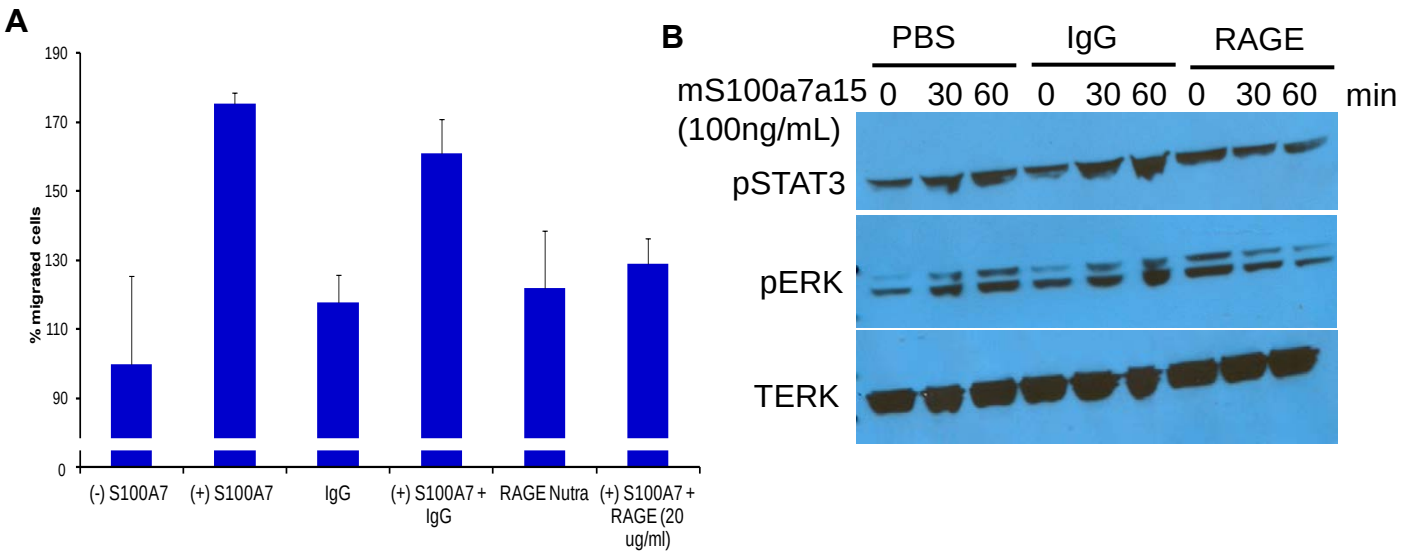


**Figure 6. Role of RAGE in chemotaxis and signaling of RAW264.7 cells.** (A) murine macrophage RAW264.7 cells were pretreated 1hour with RAGE blocking antibody or control IgG (20 μg) and 1x10$^5$ cells were plated on the top chamber of 8 μm pore polycarbonate membrane filters and medium in absence or presence of murine mS100a7a15 (100ng/mL) was placed in the lower chamber. After 12 hours of incubation, cells that migrated across the filter towards medium with or without murine mS100a7a15 (100ng/mL) were fixed, stained and counted by bright-field microscopy in five random fields. (B) MDA-MB231 cells were treated for 1 hour with RAGE blocking antibody or control IgG (20 μg) and stimulated with 100 ng/ml of recS100a7a15 for different time periods. Cell lysates were analyzed for Phospho-ERK (p-ERK), ERK and p-STAT3 by Immunoblotting.

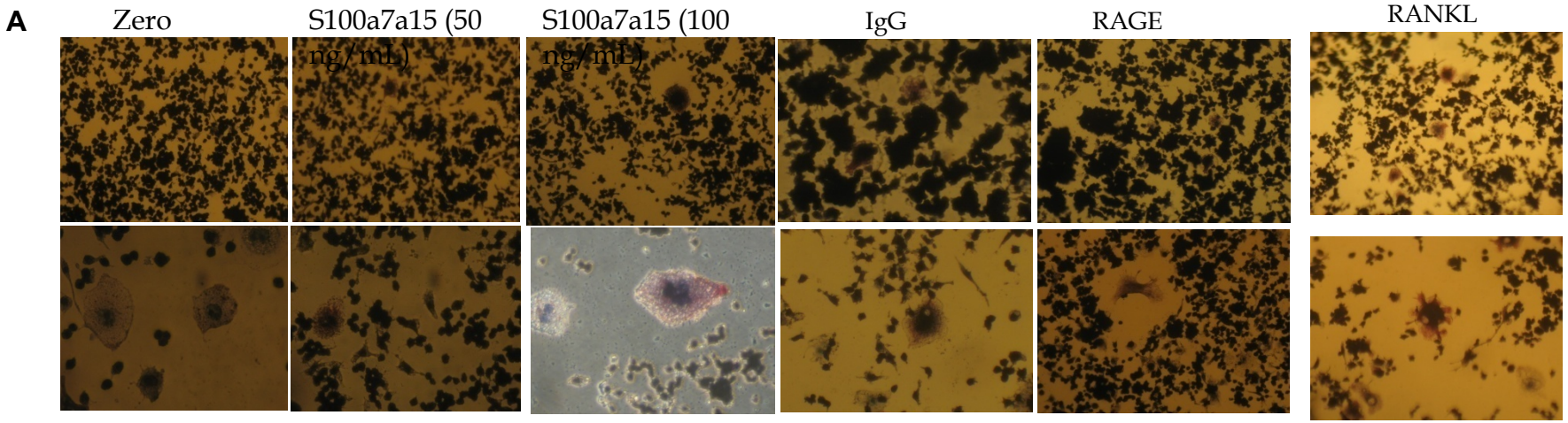


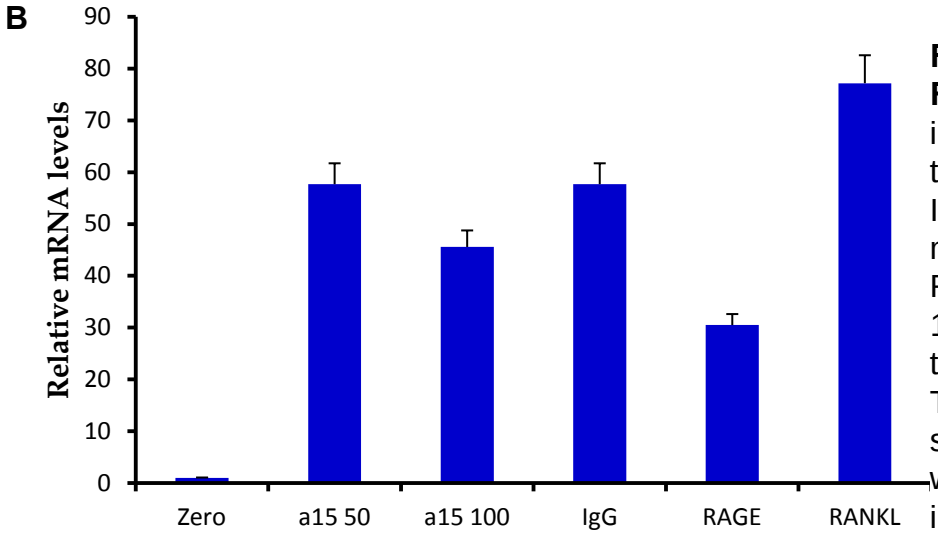


**Figure 7. RAGE regulates osteoclast formation of RAW264.7 cells.** (A) RAW 264.7 cells were incubated with or without mS100a7a15 100 ng/mL in the presence of RAGE blocking antibody or control IgG (20 μg) for 7 days and TRAP activity was measured as a marker of osteoclastic differentiation. RAW 264.7 cells grown on 6-well plate were fixed with 10% (v/v) formalin and washed with PBS. They were then incubated with solution of (p-nitrophenyl, and Tartarate) at 37°C for 30 min. After the incubation, the solution was removed from each well and Washed with distilled water and counter staining for 2 minutes in Hematoxylin. The purplish to dark brown granules, indicate the formation of TRAP. (B) number of TRAP positive cells were determined by real time PCR using gene specific primers against cathepsin K.

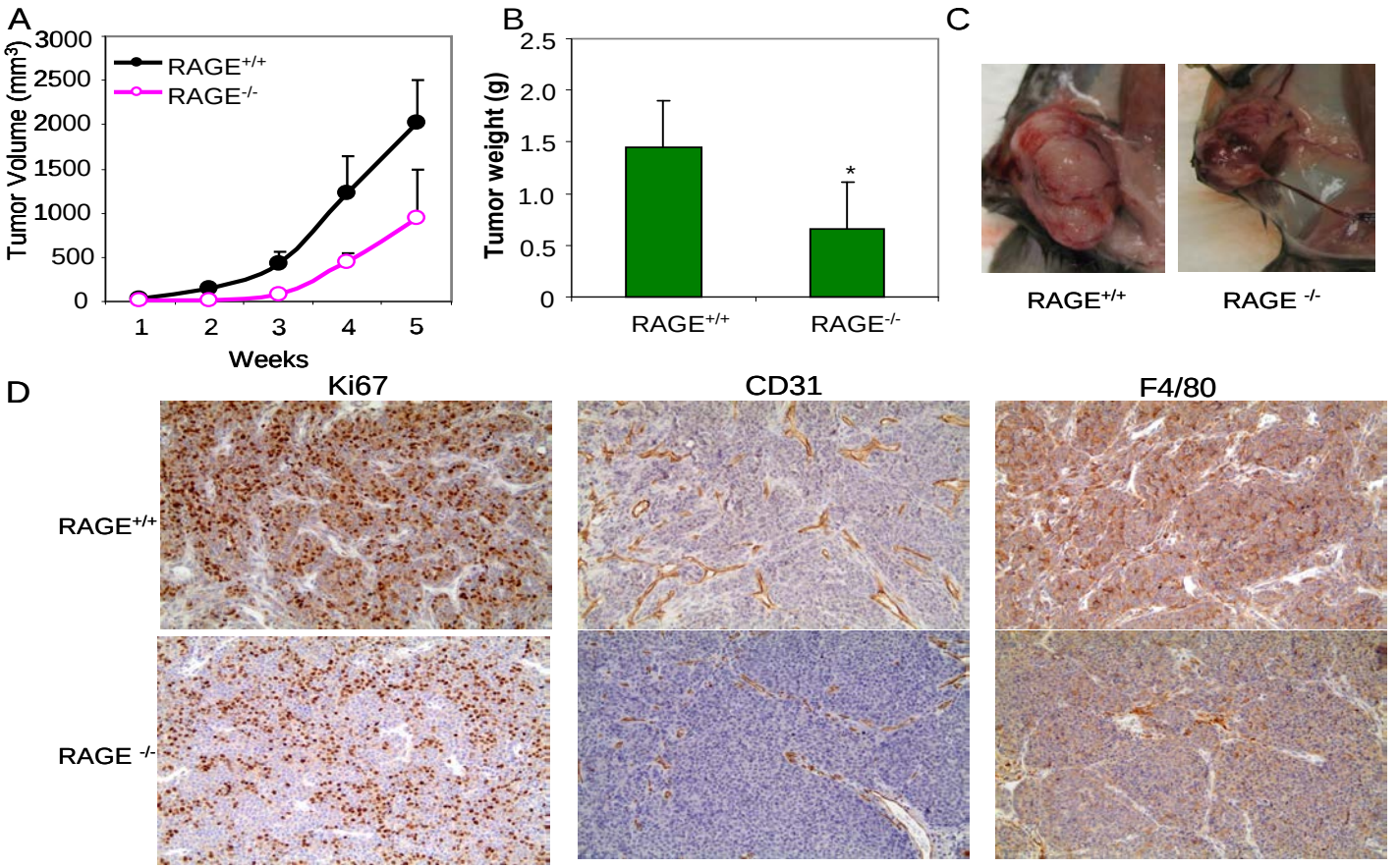


**Figure 8. RAGE deficiency inhibits tumor growth in syngenic orthotopic models.** PyMT cells ($1x10^5$) derived from MMTV-PyMT mice, were orthotopically injected into the #4 MG of the RAGE KO and wildtype C57Bl/6 mice (n=5). (A) Tumor volume was measured every week in these mice was assessed periodically and calculated using the formula length x (width)2/2. (B) Tumor weight. (C) Representative photograph of mice showing tumors dissected from different experimental groups. (D) Representative Immunohistochemical analysis with Ki67, proliferation marker, CD31, endothelial marker and F4/80, tumor associated macrophages in different experimental groups.

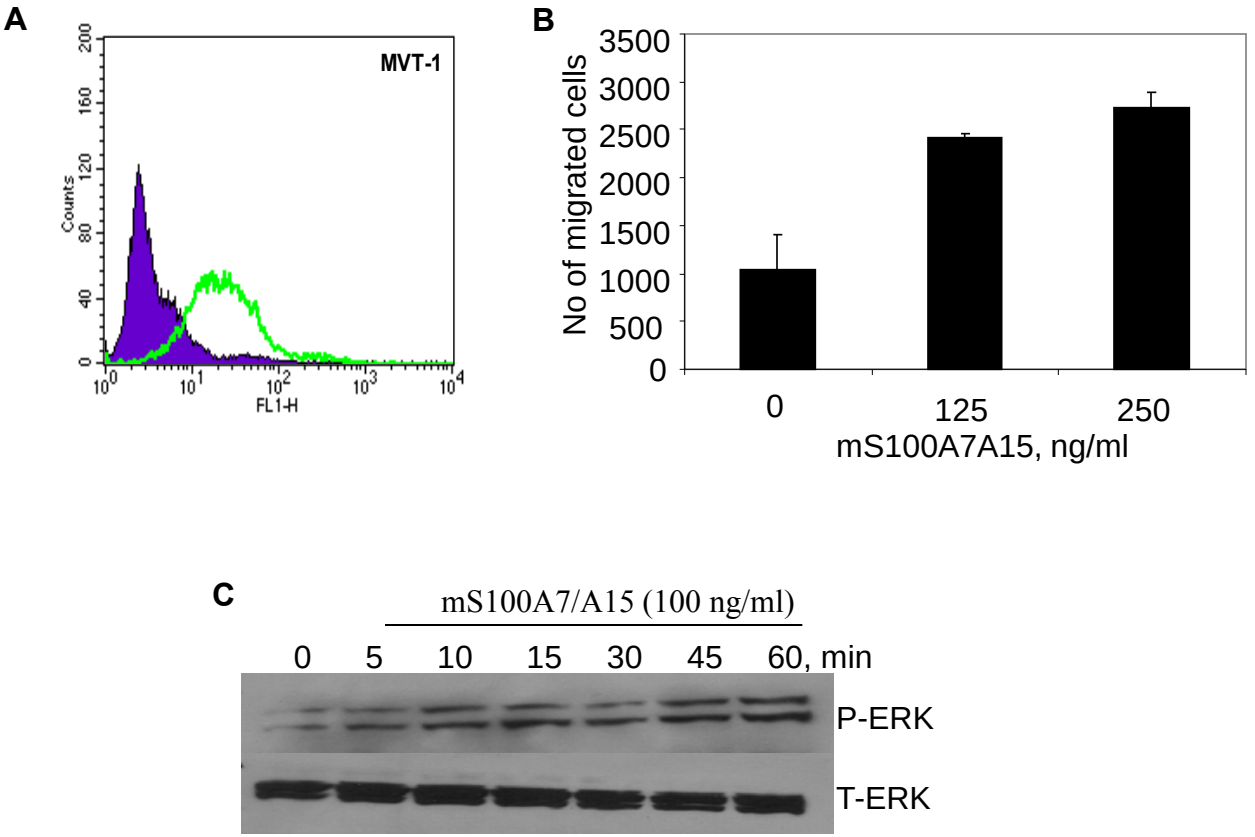


**Figure 9. soluble mS100a7a15 enhances MVT-1 migration and signaling.** (A) RAGE expression in MVT-1 cells were determined by flowcytometry (B) MVT-1 cells were subjected to a chemotaxis assay towards recombinant recombinant mS100a7a15 (125 and 250 ng/ml) using transwell plates (BD) (C) MVT-1 cells were stimulated with 100 ng/ml of recmS100a7a15 at different time points as indicated and cell lysates were analyzed for p-ERK expression by WB

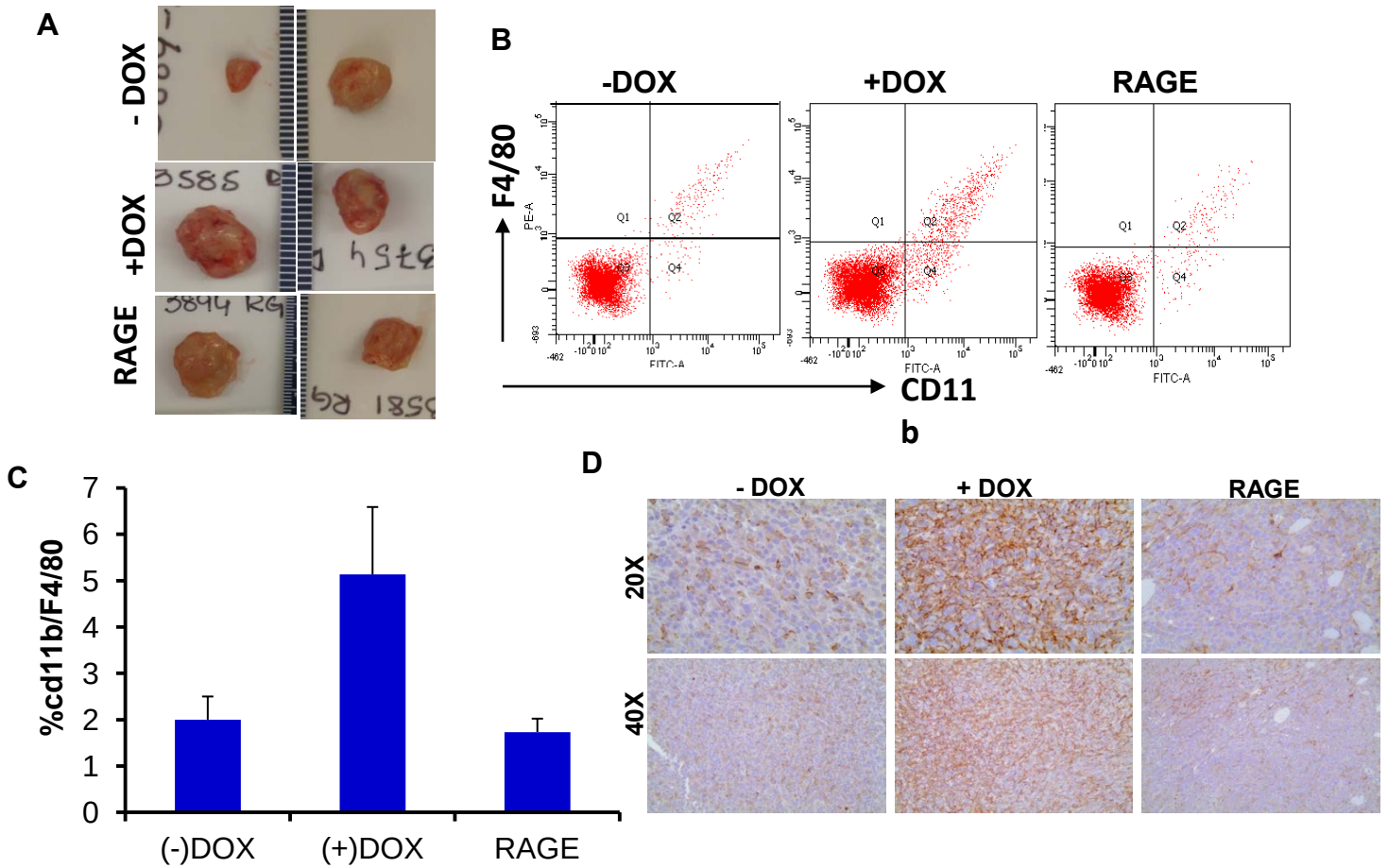


**Figure 10. RAGE Promotes Growth of Breast Tumors in orthotopic model** MVT-1 cells were injected into the mammary gland of the MMTV-mS100a7a15 mice (n =5). Five days prior to injection, mice (n=5) were fed with 1 g/kg Dox-chow to induce mS100a7a15 and mice maintained on normal diet served as control. When tumor becomes palpable, mice will be injected mice with 80 μg/kg body weight of RAGE neutralizing or IgG control antibodies every alternate day for 4 weeks. (A) representative photograph of mice showing tumors dissected from different experimental groups. (B and C) tumor cells of MVT-1 cell line derived tumors from doxycycline-treated and untreated MMTV-mS100a7a15 mice were subjected to flow cytometry for macrophage marker CD11b/F4/80 and (D) MVT-1 cell line derived tumors from doxycycline-treated and untreated MMTV-mS100a7a15 mice were subjected to immunohistochemical staining for macrophage marker, F4/80.

Breast Cancer Res Treat (2013) 138:727–739
DOI 10.1007/s10549-013-2491-4

PRECLINICAL STUDY

# Differential role of psoriasin (S100A7) in estrogen receptor α positive and negative breast cancer cells occur through actin remodeling

**Amita Sneh · Yadwinder S. Deol · Akaansha Ganju · Konstantin Shilo · Thomas J. Rosol · Mohd W. Nasser · Ramesh K. Ganju**

Received: 25 January 2013 / Accepted: 18 March 2013 / Published online: 28 March 2013


**Abstract** Psoriasin (S100A7) is a calcium-binding protein that has shown to be highly expressed in high-grade ductal carcinoma in situ (DCIS) and a subset of invasive breast cancers. However, its role in invasion and metastasis is not very well known. In this study, we have shown that S100A7 differentially regulates epidermal growth factor (EGF)-induced cell migration and invasion in ERα$^-$ MDA-MB-231 cells and ERα$^+$ MCF-7 and T47D breast cancer cells. Further signaling studies revealed that S100A7 enhances EGF-induced EGFR phosphorylation and actin remodeling that seems to favor lamellipodia formation in ERα$^-$ cells. In addition, S100A7 overexpression enhanced NF-κB-mediated matrix metalloproteinase-9 (MMP-9) secretion in MDA-MB-231 cells indicating its role in enhanced invasiveness. However, S100A7 overexpression inhibited migration and invasion of MCF-7 cells by inactivating Rac-1 pathway and MMP-9 secretion. Moreover, S100A7 overexpressing MDA-MB-231 cells showed enhanced metastasis compared to vector control in in vivo nude mice as detected by bioluminescence imaging. Our tissue microarray data also revealed predominant expression of S100A7 in ERα$^-$ metastatic carcinoma, especially in lymph node regions. Overall these studies suggest that S100A7 may enhance metastasis in ERα$^-$ breast cancer cells by a novel mechanism through regulation of actin cytoskeleton and MMP-9 secretion.

**Keywords** Breast cancer · S100A7 · Estrogen receptor-α · Actin remodeling · MMP-9

**Abbreviations**

| | |
|---|---|
| S100A7 | Psoriasin |
| ERα | Estrogen receptor α |
| EGF | Epidermal growth factor |
| DCIS | Ductal carcinoma in situ |
| IHC | Immunohistochemistry |

## Introduction

Psoriasin (S100A7) is a low molecular weight S100 gene family protein, originally isolated from skin psoriatic lesions [1]. The S100 gene family consisting of ~20 members is defined by calcium binding helix–loop–helix structural EF hand motif [2]. Apart from two calcium-binding sites, S100A7 has an additional zinc-binding site [3]. S100A7 expression has been reported in epithelial malignancies such as breast, lung, bladder, skin, esophageal, gastric, and head and neck [4–7]. In breast cancer, S100A7 expression is

Amita Sneh and Yadwinder S. Deol contributed equally to this study.

**Electronic supplementary material** The online version of this article (doi:10.1007/s10549-013-2491-4) contains supplementary material, which is available to authorized users.

A. Sneh · Y. S. Deol · A. Ganju · K. Shilo · M. W. Nasser · R. K. Ganju
Department of Pathology, The Ohio State University, Columbus, OH 43210, USA

T. J. Rosol
Department of Veterinary Sciences, The Ohio State University, Columbus, OH 43210, USA

M. W. Nasser (✉)
The Ohio State University, 840 Biomedical Research Tower, 460 W. 12th Avenue, Columbus, OH 43210, USA
e-mail: Mohd.Nasser@osumc.edu

R. K. Ganju (✉)
The Ohio State University, 810 Biomedical Research Tower, 460 W. 12th Avenue, Columbus, OH 43210, USA
e-mail: ramesh.ganju@osumc.edu

highly associated with high-grade ductal carcinoma in situ (DCIS) and invasive carcinoma compared to normal breast tissues [4, 8, 9]. Differential expression of S100A7 in breast cancer was initially observed in primary breast cancer compared to normal tissue [10]. Previous studies have shown that S100A7 is expressed in ~50 % of ERα$^-$ and only ~20 % of ERα$^+$ cases of breast cancer [4, 8, 9, 11–13]. Interestingly, in terms of prognosis, both DCIS and invasive breast cancer forms showed consistent association of S100A7 with ERα$^-$ tumors [4]. Furthermore, S100A7 has been known to modulate tumor growth by activating several signaling pathways, including PI3K, NF-κB, AP-1, and Jab1 [13–15]. However, recent studies have reported the tumor suppressive effects of S100A7 in ERα$^+$ breast cancer cells [16, 17].

Breast carcinoma is classified based on the expression of three receptors: EGFR, ER, and HER-2. EGFR expression is closely related to ER receptor status and has adverse association to overall patient survival with poor prognosis. One prominent feature of ERα$^-$ tumors, especially triple-negative basal-like subtype, is the expression of EGFR [18]. These basal-like tumors are associated with aggressive histological features, poor prognosis and are extremely difficult to treat. High EGFR expression is also associated with metastatic and invasive form of breast cancer [18]. EGFR activation provokes a plethora of signaling pathways that includes cell proliferation, adhesion and motility and promotes invasion and angiogenesis [19]. Recent studies in our laboratory and others have shown that S100A7 regulates epidermal growth factor (EGF)/EGFR-mediated signaling pathways [13–15]. Studies have also shown that S100A7 and EGFR are associated with ERα$^-$ tumors in a large unselected cohort of breast cancer patients [13].

Actin dynamics and remodeling have been identified as major determinant of metastasis and invasion that are the key basis of most cancer-related deaths. During cell motility, branched network of actin filaments are required to assemble beneath the plasma membrane to consistently progress the cell forward to form lamellipodia [20]. The recruitment of active Rac1, a small Rho GTPase at the leading edge, is itself sufficient for cell extension and further movement [21, 22]. Moreover, the influence of S100A7 in calcium-mediated signal transduction and cellular events through direct interactions with intermediate filaments also implies its role in modulation of the cytoskeleton [2].

Hence, present study investigated the influence of S100A7 on metastatic and invasive abilities of ERα$^-$ and ERα$^+$ breast cancer cells upon EGF stimulation. Our studies showed that S100A7 differentially regulates migration and invasion in ERα$^-$ and ERα$^+$ cells. S100A7 overexpression enhanced EGF-induced migration/invasion in ERα$^-$ cells, while its overexpression inhibited migration/invasion in ERα$^+$ cells. We also showed that S100A7 enhances metastasis in vivo and its predominant expression was observed in ERα$^-$ lymph node metastatic group of breast patient samples. In addition, actin polymerization pathway seems to play an important role in establishing the differential effect of S100A7 in ERα$^-$ and ERα$^+$ breast cancer cells.

## Materials and methods

### Cells, stable transfections, and antibodies

The vector information and generation of stable clones of MDA-MB-231, MCF7, and T47D breast carcinoma cells with stable vector and S100A7 overexpression used in the present study are as described earlier [16, 23]. Knockdown of p65-NF-κB was performed using its siRNA transfection (50 nM; Dharmacon) for 72 h using lipofectamine 2000 as per manufacturer's protocol. Antibodies used were mostly from Cell Signaling, GAPDH (Santa Cruz Biotechnology) and Phalloidin-568 (Invitrogen).

### Migration and invasion assay

Wound healing assay, chemotaxis assay, and invasion assay were performed and calculated as described previously [15, 16, 23, 24].

### Gelatin zymography

This method was used to compare MMP-2 and MMP-9 with gelatinase activity of MDA-MB-231 and MCF-7 cells upon S100A7 overexpression (24 h). Supernatants containing secreted form of MMPs were concentrated using centrifugal filter units (Millipore) and detected using Novex gelatin zymography. Renaturing, developing, and staining steps were followed to visualize active MMP bands according to the manufacturer's instructions (Life technologies).

### Western blotting

Western blot analysis was done as previously described [23, 24].

### Rac1 activation assay

Activation of Rac1 was determined using the Rac/Cdc42 activation assay kit as per manufacturer's protocol (Millipore). Briefly, cell lysates were incubated with 10 μg/mL p21-activated kinase 1 agarose beads for 60 min at 4 °C. Agarose beads were collected by centrifugation followed by heat denaturation of samples and Rac1 activation was

evaluated by immunoblotting by anti-human Rac1 antibody.

### G-actin/F-actin in vivo biochemical assay

This quantitative assay was performed to determine the relative effect of EGF on filamentous actin (G-actin) versus free globular actin (F-actin) content. Briefly, cells were suspended in F-actin stabilizing buffer and separated from G-actin by ultra-centrifugation as per manufacturer's directions (Cytoskeleton Inc.). The difference in G-actin and F-actin content was examined by western blot using G-actin antibody.

### Confocal microscopy

Briefly, treated cells were fixed with 4 % paraformaldehyde at room temperature. Cells were washed with 1× PBS, blocked with 5 % BSA in 1× PBS for 60 min and incubated with Phalloidin-568 overnight at 4 °C. Cells were washed with 1× PBS and mounted using vectashield mounting medium containing DAPI and examined under Olympus FV1000 Filter confocal microscope. Images were acquired with 40× objective and modified using FV10-ASW2.0 software.

### Bioluminescent imaging (BLI) and analysis

Nude mice obtained from Charles River Laboratories, were maintained at Ohio State University animal facility under IACUC rules and regulations. Nude mice ($n = 10$) were injected intracardially with MDA-MB-231-luc-D3H2LN-S100A7-luciferase or vector control ($1 \times 10^5$/100 μL) and were weekly assessed for tumor burden (IVIS System 200, Xenogen Corporation). Mice were anesthetized intraperitoneally with 0.15 mg/mL of D-luciferin (PBS) and bioluminescent images were collected between 2 and 5 min post-injection. The light intensity was detected by IVIS camera system, integrated, digitalized, and displayed for relative photon flux as calculated per mouse.

### Tissue microarrays (TMA) and immunohistochemical analysis

TMA were obtained from Imgenex (San Diego, CA) and immunohistochemistry (IHC) analysis was performed on paraffin-embedded formalin fixed breast tissue specimens. TMAs were de-paraffinized according to manufacturer's recommendation and immunostained with S100A7 antibody at 1:50 dilution (Imgenex). Vectastain Elite ABC reagents (Vector Laboratories) using avidin DH:biotinylated horseradish peroxidase H complex, 3,3′-diaminobenzidine (Polysciences), and Mayer's hematoxylin (Fisher Scientific) were used for detection of the bound antibodies.

### Statistical analysis

All the experiments were performed at least three to four times to confirm the results. The results were then expressed as mean ± SD of data obtained from these three or four experiments. The statistical significance was determined by the Student's $t$ test and value of $p < 0.05$ was considered significant as denoted by asterisks.

## Results

### S100A7 overexpression differentially activates EGFR in ERα$^-$ and ERα$^+$ breast cancer cells

It has been shown that S100A7 downregulation inhibits EGFR-mediated signaling in ERα$^-$ cells [15]. Here, we have analyzed the effect of S100A7 overexpression on EGF-induced receptor activation in ERα$^-$ (MDA-MB-231) and ERα$^+$ (MCF-7 and T47D) cells by EGFR phosphorylation. We observed an increase in EGFR phosphorylation in S100A7 overexpressing MDA-MB-231 cells upon EGF treatment (Fig. 1a). However, S100A7 overexpression reduced EGF-induced EGFR phosphorylation in MCF7 cells compared to vector (Fig. 1b). In another ERα$^+$ cell line, T47D, we observed similar results of time-dependent inhibition of EGFR phosphorylation upon EGF stimulation (Fig. 1c). The quantitative analysis of all immunoblots showed consistent increase and decrease in EGFR phosphorylation of S100A7 overexpressing ERα$^-$ and ERα$^+$ cells, respectively (Fig. 1d–f). Therefore, differential EGFR phosphorylation might play an important role in S100A7 overexpressing ERα$^-$ and ERα$^+$ breast cancer cells.

### S100A7 overexpression affects cell motility of ERα$^-$ and ERα$^+$ cells

The motile ability of tumor cells determines their metastatic phenotype. In the present study, EGF-induced cell migration was performed to analyze the cell motility of ERα$^-$ and ERα$^+$ cells upon S100A7 overexpression. The wound healing assay revealed the effect of S100A7 in directional cell migration of ERα$^-$ and ERα$^+$ cells. The assay showed S100A7 to significantly increase EGF-mediated migratory abilities of S100A7 overexpressing MDA-MB-231 cells (Fig. 2a). We observed significant increase in wound closure of S100A7 overexpressing MDA-MB-231 cells compared to vector control. In contrast, S100A7 inhibited the directional cell migration of ERα$^+$ MCF-7

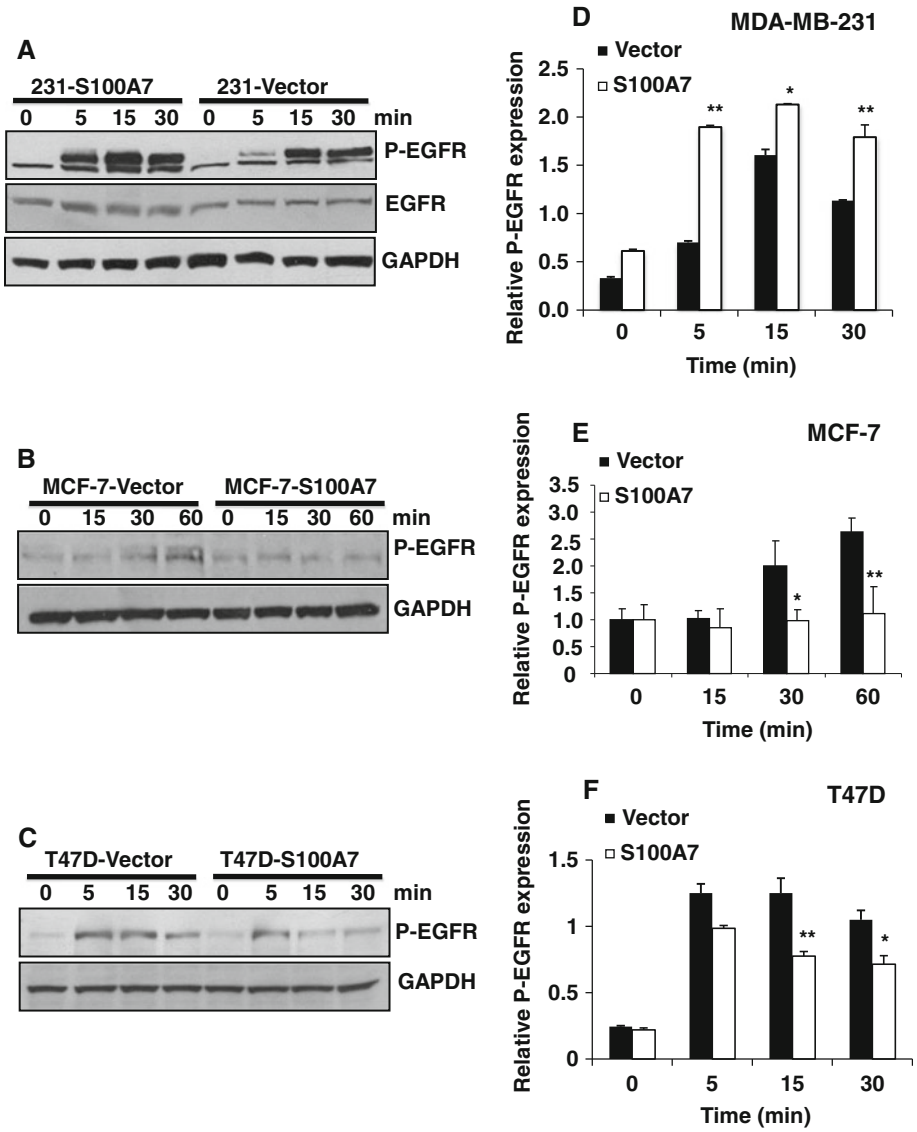


**Fig. 1** EGF-induced differential phosphorylation of EGFR in ERα$^-$ and ERα$^+$ breast cancer cells with S100A7 overexpression. EGFR phosphorylation status was analyzed in S100A7 overexpressing ERα$^-$ MDA-MB-231 cells (**a**) and ERα$^+$ MCF-7 (**b**) and T47D cells (**c**) on EGF stimulation (100ng/mL) by western blotting. The relative EGFR phosphorylation levels in all cells are representative of three independent experiments, calculated with respect to GAPDH for MDA-MB-231, MCF-7, and T47D (**d**–**f**) at indicated time. The statistically significant *p* values were indicated as *<0.05 and **<0.005

cells by relatively slowing down their wound closure compared to vector cells (Fig. 2b). Moreover, cell migration assay using transwell chambers showed ∼five fold increase in EGF-induced migration of S100A7 overexpressing MDA-MB-231 cells compared to its vector control (Fig. 2c). SCP6, a single cell progeny of MDA-MB-231 cells, which has previously been characterized as a low metastatic cell line, was also analyzed to evaluate the effect of S100A7 overexpression on cell migration (Supplementary Fig. 1a) [25]. Importantly, S100A7 was able to promote EGF-induced cell migration in SCP6 as well. However, S100A7 overexpression in MCF-7 cells inhibited EGF-induced cell migration by ∼eight fold (Fig. 2d). Similar results were seen on S100A7 overexpression in ERα$^+$ T47D cell line, which showed lesser inhibition in cell migration compared to MCF-7 cells (Supplementary Fig. 1b). Taken together, these data reveal the differential consequence of S100A7 on migratory response of breast cancer cells depending on their ERα status.

## Role of MMP-9 activation in invasiveness of S100A7 overexpressing ERα$^-$ and ERα$^+$ cells

One of the hallmarks of tumor metastasis is its ability to degrade extracellular matrix to invade distant organs. Matrigel invasion assay was performed to analyze the EGF-induced invasion of S100A7 overexpressing ERα$^-$ and ERα+ cells. We found that S100A7 overexpression has significantly increased EGF-induced invasive ability of MDA-MB-231 cells compared to vector control by approximately twofold (Fig. 3a). However, there was a considerable decrease in invaded population of S100A7 overexpressing MCF7 cells upon EGF stimulation (Fig. 3b). Similar EGF-mediated inhibition of cell invasion

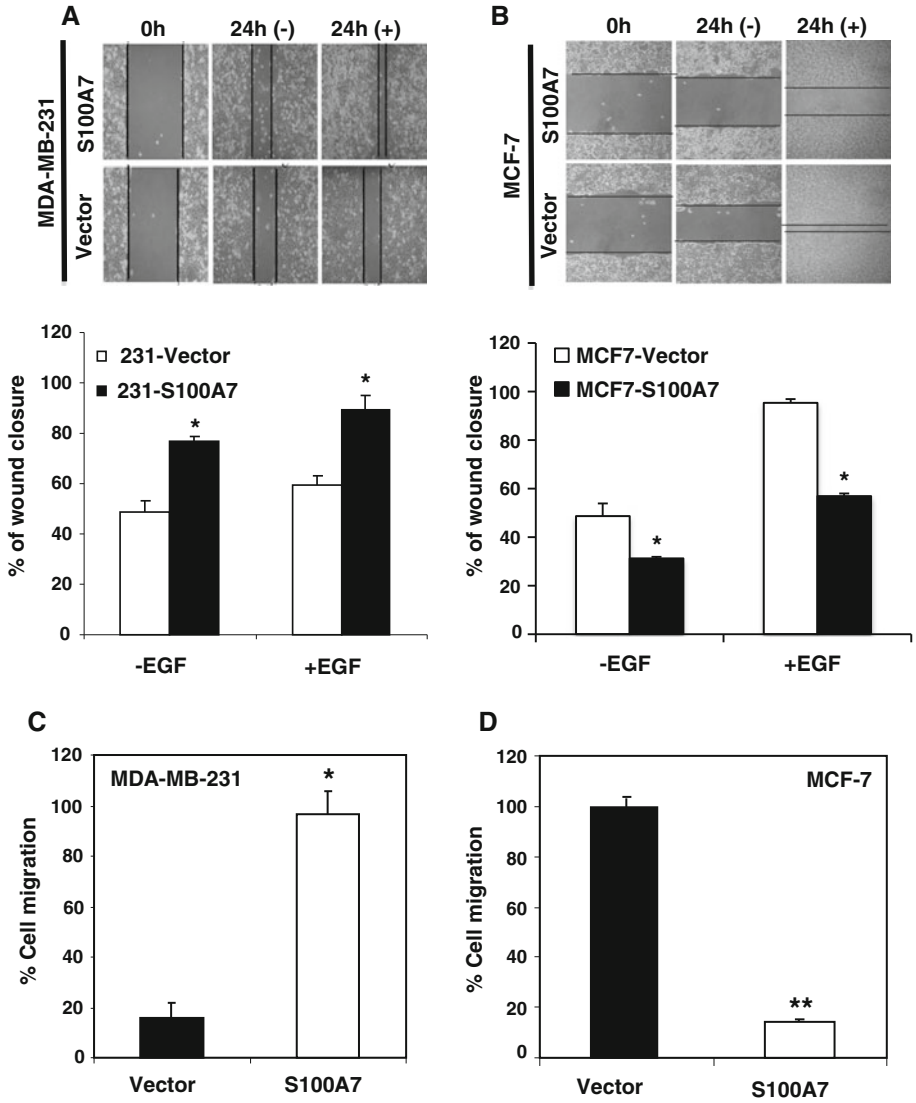


**Fig. 2** Effect of S100A7 on EGF-induced cell motility, migration, and invasion of ERα$^-$ and ERα$^+$ cells. Wound healing assay images represent EGF-induced effect on cell motility of S100A7 overexpressing MDA-MB-231 and MCF-7 cells compared to their vector control (**a**, **b**). Their quantitative analysis represent one of the three independent experiments performed with *p* value denoted as *<0.05. Relative migratory potential of S100A7 overexpression in MDA-MB-231 (**c**) and MCF-7 cells (**d**) was compared to vector by transwell migration assay, represented as percent cell migration with *P* value as *<0.05 and **<0.005. EGF-induced effects were analyzed at 100ng/mL concentration for cell motility assays

was observed in S100A7 overexpressing T47D cells compared to control cells (Supplementary Fig. 2). The difference in invasion of vector and S100A7 overexpressing cells has been expressed as percentage, which was statistically significant. It is known that cancer cells require matrix metalloproteinases (MMPs) to invade the extracellular matrix underlying their basement membrane and stroma. Hence, we have analyzed the presence of S100A7 expression on activation status of MMP-2 and -9 that have implications in the process of tumor invasion [26]. We observed an increase in active form of MMP-9 secretion in S100A7 overexpressing MDA-MB-231 cells, while its activity was decreased in S100A7 overexpressing MCF7 cells (Fig. 3c, d). However, the MMP-2 activation was not affected in both vector and S100A7 overexpressing MDA-MB-231 and MCF-7 cells. Therefore, diverse MMP-9 activation in S100A7 overexpressing MDA-MB-231 and MCF7 cells suggests the significance of MMP-9 in S100A7 associated invasiveness.

## Role of NF-κB in S100A7-mediated MMP-9 secretion in ERα$^-$ cells

It is known that NF-κB binding on MMP-9 gene regulates TNF-α-mediated MMP-9 secretion [27]. It has also been reported that S100A7 promotes pro-survival pathways in ERα$^-$ cells through Akt-mediated NF-κB activation [14]. Since, S100A7 regulates NF-κB activation in ERα$^-$ cells, we sought to see the effect of NF-κB knockdown on MMP-9 secretion in S100A7 overexpressing MDA-MB-231 cells. We observed a significant NF-κB downregulation in S100A7 overexpressing MDA-MB-231 cells (Fig. 3e, f). Active MMP-9 secretion was significantly reduced in NF-κB-knocked-down cells compared to scramble siRNA

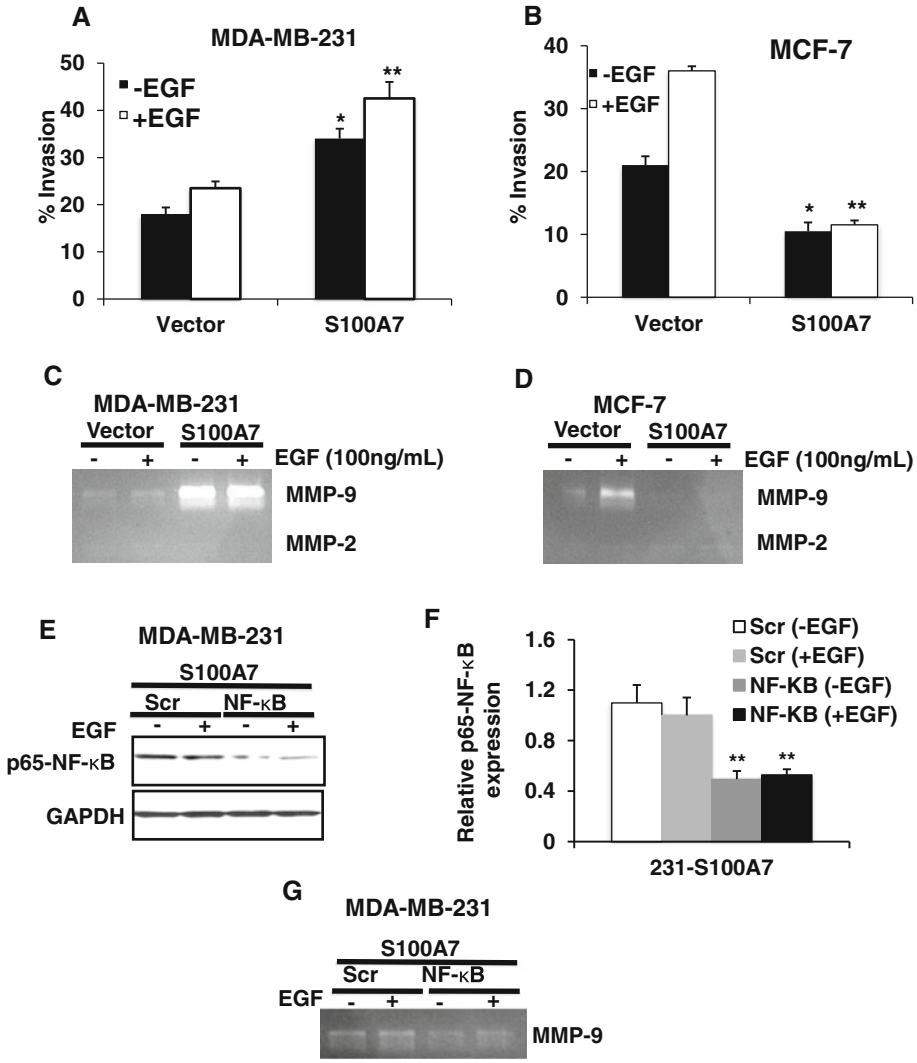


**Fig. 3** Role of NF-κB in S100A7-mediated MMP-9 secretion in ERα$^-$ and ERα$^+$ cells. The effect of EGF on relative invasiveness of MDA-MB-231 (**a**) and MCF-7 cells (**b**) on S100A7 overexpression was analyzed by matrigel invasion assay and represented as percent invasion with $p$ value <0.05 as * and <0.005 as **. Gelatin zymography revealing the level of MMP-9 secretion in MDA-MB-231 cells (**c**) and MCF-7 cells (**d**) upon S100A7 overexpression without any effect on MMP-2 levels. Images represent one of the three independently performed experiments. Knockdown of p65-NF-κB subunit (**e**, **f**) markedly inhibited the MMP-9 secretion of MDA-MB-231 cells analyzed by gelatin zymography (**g**). Images represent one of the three experiments and their quantitative analyses were statistically significant with $p$ value *<0.05 and **<0.005. Where, EGF used was 100ng/mL and *Scr* stands for scramble siRNA

control indicating the direct role of NF-κB in S100A7-mediated MMP-9 secretion (Fig. 3g).

## In vivo metastatic potential of S100A7 overexpressing MDA-MB-231 cells and clinicopathological S100A7 expression analysis in breast carcinomas

Since, S100A7 overexpression in breast cancer cell lines has been shown to enhance tumor growth [12], we investigated its significance in metastasis in vivo. In this study, we have used IVIS imaging system to analyze the metastatic potential of S100A7 overexpressing MDA-MB-231 with luciferase reporter gene (Fig. 4a). Higher metastatic progression with elevated radiation flux was observed in intracardially injected nude mice with S100A7 overexpressing MDA-MB-231 cells compared to vector control (Fig. 4b). This demonstrates that S100A7 plays an important role in promoting metastatic phenotype of ERα$^-$ breast cancer cells. Furthermore, we have analyzed the S100A7 expression in a cohort of breast tissue specimens using tissue microarray ($n = 59$). The TMA and IHC data has been summarized as in Supplementary Table 1. Our study revealed that S100A7 expression was highly prevalent in metastatic tumors, especially at lymph node region (Fig. 4c). Ninety percent of metastatic tumors showed good expression of S100A7, while normal breast tissues ($n = 9$) were devoid of S100A7 protein. Interestingly, S100A7 expressing lymph node metastatic group were mostly ERα negative. In addition, we observed predominant S100A7 expression in ERα$^-$ (~54 %) and PR$^-$ (~50 %) compared to ERα$^+$ type (~36 %) and PR$^+$ (~44 %) among 35 infiltrating ductal carcinoma carcinomas (Fig. 4d). Hence, the considerable role of S100A7 as a regulator of breast cancer metastasis seems to be directly linked to ERα status.

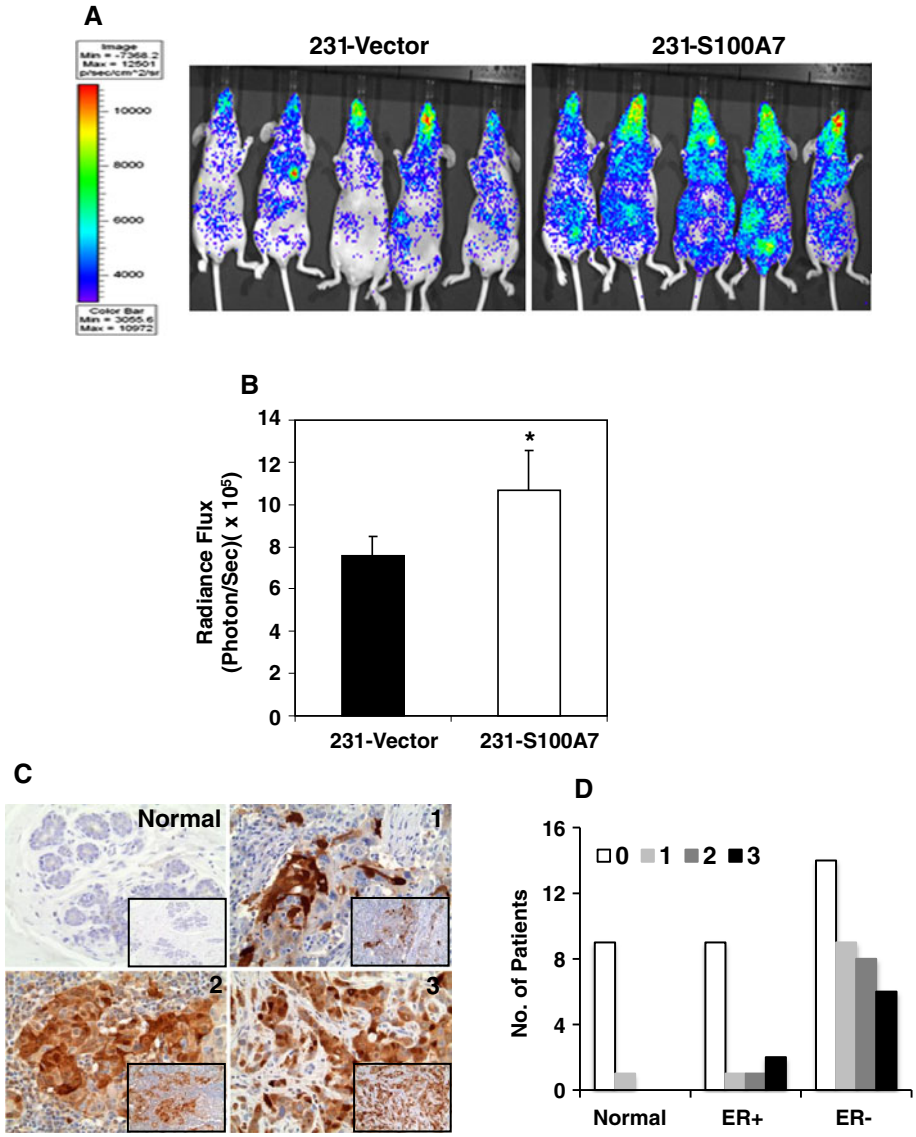


**Fig. 4** In vivo metastatic potential of S100A7 in ERα$^-$ cells and its association with ERα status. Representative BLI images show comparative metastases of control and S100A7 overexpressing MDA-MB231-luc-D3H2LN cells in nude mouse model (**a**), while the statistically significant high radiance flux was observed in the presence of S100A7 with $p$ value <0.05 (**b**). Representative immunohistochemistry images show different levels of S100A7 staining pattern in lymph node region of metastatic tissue specimens compared to normal tissue, as a negative control (**c**). Based on clinico-pathologist analysis, the overall S100A7 expression levels were quantitatively represented in ERα$^-$ and ERα$^+$ cells compared to normal breast tissues (**d**). Where 0, 1, 2, and 3 represent different S100A7 expression levels

## Role of S100A7 overexpression on actin polymerization

Actin polymerization is a well-known process that drives cell migration with the most evident feature of lamellipodia formation at leading edges of motile cells. Our immunofluorescence studies showed increased actin accumulation at the leading edges of S100A7 overexpressing MDA-MB-231 cells compared to vector upon EGF stimulation (Fig. 5a). However, there was comparatively lesser actin accumulation at the leading edges of S100A7 overexpressing MCF7 cells compared to vector control. Instead, actin seems to be distributed as small actin-filament structures that became more prominent in vector compared to S100A7 overexpressing MCF-7 cells on EGF treatment (Fig. 5b). Actin accumulation at leading edges might be responsible for differential migratory response of S100A7 in ERα$^-$ and ERα$^+$ breast cancer cells. Hence, a direct relationship between activity of actin polymerization and formation of migratory structures could be possible.

## S100A7 overexpression affect EGF-induced Rac1 activation and associated signaling

In order to investigate the role of actin polymerization pathway in S100A7-mediated differential effect in ERα$^-$ and ERα$^+$ cells, we have analyzed the activity status of Rac1, which is a key molecule in actin polymerization. Rac1 pathway is downstream of LIMK1/2 and mediates its activation through intermediate kinases like PAK1 [28]. We observed that Rac1 activity was enhanced along with LIMK1/2 expression in S100A7 overexpressing MDA-MB-231 cells compared to vector control cells at

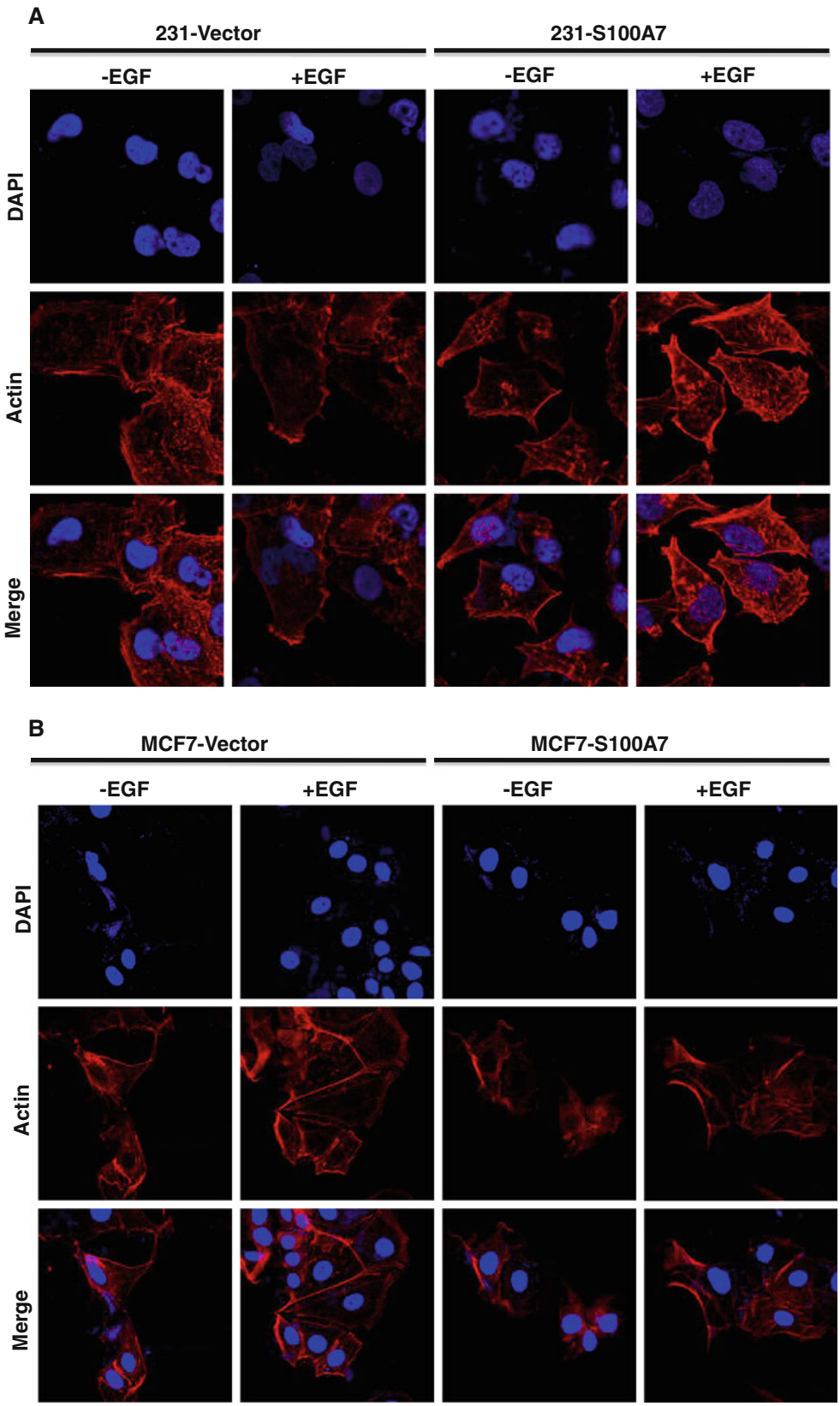


**Fig. 5** Effect of EGF on actin polymerization of S100A7 overexpressing ER$\alpha^-$ and ER$\alpha^+$ cells. Immunofluorescence images showing EGF-induced consequences on actin-based cell protrusions of MDA-MB-231 (**a**) and MCF-7 cells (**b**) on S100A7 expression. Images represent one of three independent experiments with phalloidin-568 and DAPI staining as indicated at 100ng/mL of EGF treatment

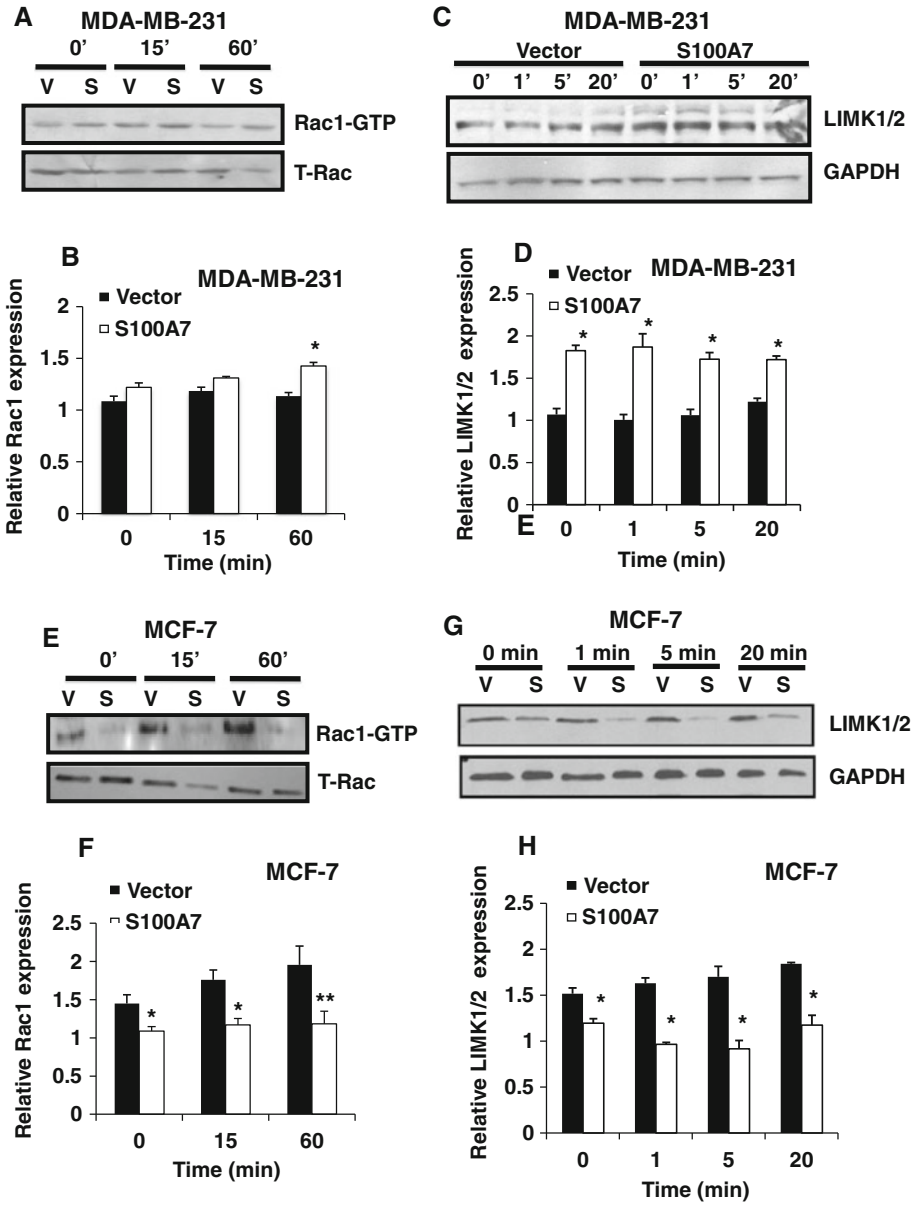


**Fig. 6** Rac-1 signaling in EGF-induced cell motility of S100A7 overexpressing ERα$^-$ and ERα$^+$ cells. Actin regulators, Rac-1 and LIMK1/2 activation status were evaluated on EGF stimulation (100ng/mL) in S100A7 overexpressing MDA-MB-231 (**a**, **c**) and MCF-7 cells (**e**, **g**) by western blot. Their quantitative analysis corresponds to three independent repeats as indicated by *asterisks* * and ** with significant $p$ value <0.05 and <0.005, respectively (**b**, **d**, **f**, **h**). Where, *V* stands for vector and *S* stands for S100A7

all time points (Fig. 6a, c). However, Rac1 activation was inhibited in MCF-7 cells on S100A7 overexpression and even EGF stimulation did not affect its activity suggesting the importance of Rac1 pathway (Fig. 6e, f). We also observed the downregulated expression of LIMK1/2 upon EGF treatment in S100A7 overexpressing MCF7 cells compared to vector control cells (Fig. 6g, h). Consistently enhanced Rac1 activity and LIMK1/2 expression reveal Rac-1 pathway as a modulator of increased migration and metastasis in S100A7 overexpressing MDA-MB-231 cells. However, Rac1 appears to act as a negative regulator in cell migration of S100A7 overexpressing MCF-7 cells.

S100A7 overexpression affects cofilin

Cofilin is one of the downstream molecules of actin polymerization that directly has impact on cell motility through activation of actin-filament dynamics. Cofilin is de-phosphorylated upon Rac1 activation and leads to the polymerization of the F-actin filaments and lamellipodium formation [29]. Our results showed time-dependent decrease in phosphorylation of cofilin in S100A7 overexpressing MDA-MB-231 cells on EGF stimulation compared to vector control cells (Fig. 7a, b). Since p-cofilin is an inactive form of cofilin, its declined level leads to increased actin polymerization–depolymerization and enhanced lamellipodium

formation as migratory structures in S100A7 overexpressing MDA-MB-231 cells seen in our immunofluorescence studies. This effect was not seen on cofilin phosphorylation in MCF7 cells upon S100A7 expression suggesting the effect of inactive Rac1 pathway and cofilin on slow mobility of S100A7 overexpressing ERα$^+$ cells (Fig. 7c, d). Hence, actin-associated regulatory pathway appears to play an important role in migratory potential of S100A7 in ERα$^-$ and ERα$^+$ breast cancer cells.

S100A7 regulated EGF-induced actin turnover

So far, our studies suggest that S100A7-mediated cell motility is controlled by actin polymerization and associated downstream signaling. However, actin-filament subunits (F-actin) need to be recycled back to monomeric forms (G-actin) to maintain further polymerization and motility [30]. Hence, the influence of S100A7 associated actin polymerization on G-actin/F-actin content upon EGF stimulation was examined by an in vivo assay kit. The assay showed more G-actin content with decreased F-actin quantity in S100A7 overexpressing MDA-MB-231 cells on EGF stimulation (Fig. 7e). The decrease in F-actin and simultaneous increase in G-actin content might be responsible for enhancing ATP based actin recycling during actin polymerization, thus significantly enhancing actin turnover with time. Moreover, there was no effect of EGF on F-actin and G-actin content on S100A7 overexpression in MCF7 cells (Fig. 7f). The diverse influence of EGF on G-actin/F-actin content and actin turnover in S100A7 overexpressing ERα$^-$ and ERα$^+$ cells significantly correlated with the activation of actin polymerization pathway.

## Discussion

In this study, we report for the first time that S100A7 differentially regulates EGF-induced EGFR phosphorylation

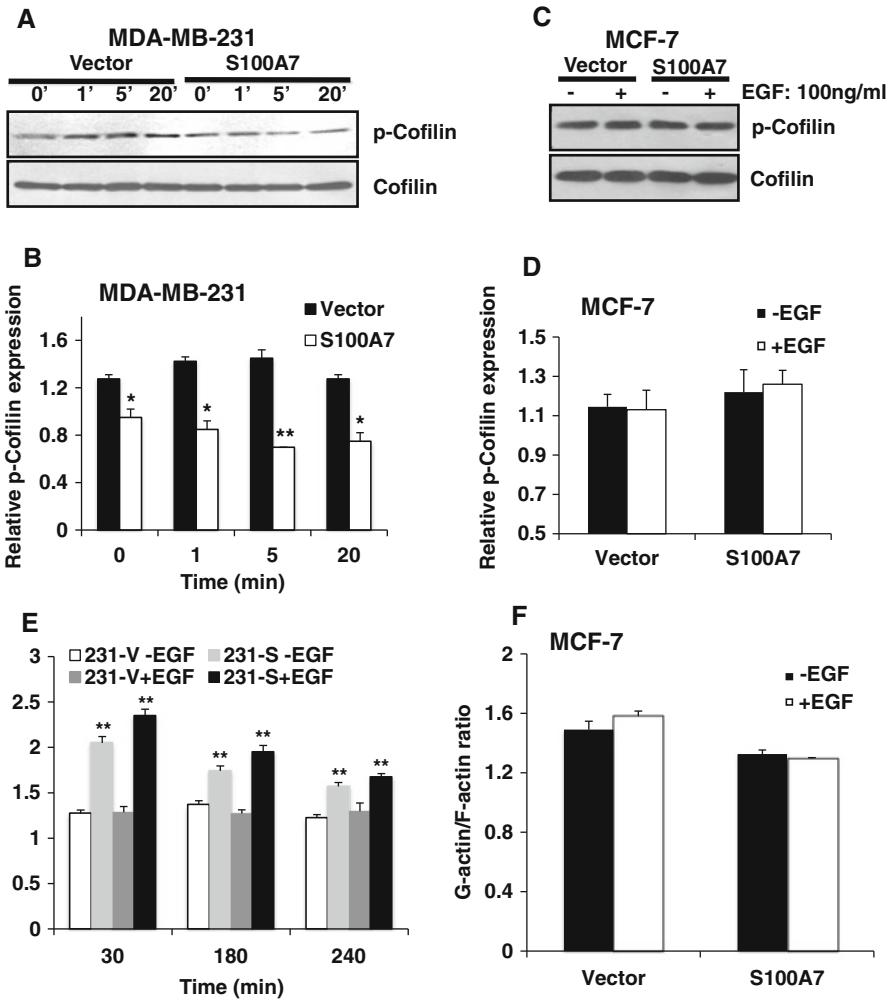


**Fig. 7** Role of Cofilin signaling on actin remodeling of S100A7 overexpressing ERα$^-$ and ERα$^+$ cells. Phosphorylation status of cofilin as a negative actin regulator was assessed to show effect of EGF on S100A7 overexpressing MDA-MB-231 (**a**) and MCF-7 cells (**c**). The relative phosphorylation levels appear to be significant with $p$ value *<0.05 and **<0.005 (**b**, **d**). Effect of EGF-induced actin regulation in S100A7 overexpressing MDA-MB-231 (**e**) and MCF-7 (**f**) cells were quantitatively evaluated by in vivo actin turnover assay as a change in G-actin/F-actin ratio over the indicated time. Where EGF used was 100 ng/mL

and migration of ERα$^-$ and ERα$^+$ breast cancer cells. We observed an increase in EGFR phosphorylation in S100A7 overexpressing ERα$^-$, whereas reduced EGFR phosphorylation was seen in ERα$^+$ cells. The estrogen receptor pathway is known to crosstalk with EGFR pathway and since S100A7 negatively regulates ER, it could be possible that S100A7 may likely inhibit EGF activity in ERα$^+$ cells [13, 16]. However, EGF-induced downregulation of EGFR phosphorylation in S100A7 overexpressing ERα$^+$ cells could also be due to the downregulation of β-catenin/TCF4 pathway shown in previous studies [16, 31]. Therefore, it is reasonable to mention that S100A7-mediated differential EGF receptor activation appears to be regulated through different pathways in ERα$^-$ and ERα$^+$ cells.

Increased invasive and migratory properties are important characteristics of metastatic breast cancer cells. Our previous studies on MVT-1 orthotopic syngeneic bi-transgenic mS100a7a15 mouse model showed enhanced metastasis through M2-macrophage recruitment [23]. EGF/EGFR-axis is known to regulate cell spreading, motility and invasion through extracellular matrix (ECM). In this study, we demonstrate EGF-induced increase in migration and invasion of S100A7 overexpressing MDA-MB-231 cells. In addition, our in vivo nude mouse model study revealed that S100A7 is associated with increased metastatic capacity of ERα$^-$ cells. Furthermore, our studies revealed that S100A7 enhanced NF-κB-mediated MMP-9 secretion in MDA-MB-231 cells. MMP-9 has been shown to play an important role in breast cancer invasion and metastasis [32]. Consistent with our studies, other S100 gene family proteins also promote tumor metastasis through MMP's activation [33, 34]. Our patient sample data also suggest that S100A7 is widely expressed in metastatic carcinoma, especially in lymph node regions. Interestingly, all S100A7 expressing metastatic samples were ERα negative providing further evidence of S100A7 involvement in ERα$^-$ tumor metastasis. However, S100A7-mediated effects on cell migration and invasion were inhibited in ERα$^+$ breast cancer cells with decreased MMP-9 activity.

Metastasis is a multi-step process which can be driven by several ways such as actin polymerization, cell adhesion, and acto-myosin contraction [35]. Hence, we have analyzed the influence of S100A7 in ERα$^-$ and ERα$^+$ cells on actin polymerization pathway, which has been extensively studied in cancer metastasis. We revealed an increase in actin polymerization in MDA-MB-231 cells and decrease in MCF7 cells on S100A7 overexpression compared to vector control. Furthermore, we have shown that increased actin polymerization in S100A7 overexpressing ERα$^-$ cells is due to more lamellipodia formation at leading edges that is regulated by Rac1 pathway. Rac1 has been shown to control cofilin phosphorylation through the activity of class II PAKs that is regulated through LIM kinases and other downstream effectors of the Rho family of GTPases, Cdc42, Rac, and Rho [36]. Our results suggest that S100A7 overexpression in ERα$^-$ cells downregulates cofilin phosphorylation with increased LIMK1/2 expression. This can increase the number of barbed ends available during directional cell movement [28, 36]. Therefore, increased LIMK1/2 and cofilin dephosphorylation mediates enhanced directional migration of S100A7 overexpressing ERα cells. However, downregulated LIMK1/2 expression and presence of inactive phosphorylated form of cofilin appears to inhibit local actin polymerization at leading edges and reduced EGF-induced migration in S100A7-overexpressing ERα$^+$ cells. Interestingly, prominent cytoplasmic staining of actin filaments in S100A7 overexpressing MDA-MB-231 cells on EGF stimulation could be explained by increased actin turnover. Our in vivo G-actin/F-actin assay demonstrates that G-actin/F-actin ratio regulates actin turnover, which is maintained by S100A7-mediated activation of Rac1 pathway on EGF stimulation in MDA-MB-231 cells. However, ineffective actin turnover in MCF-7 cells could be due to inhibited actin regulatory Rac1 pathway.

In summary, our proposed model describes the EGF-induced differential role of S100A7-mediated actin remodeling and MMP-9 in ERα$^+$ and ERα$^-$ breast cancer cells (Supplementary Fig. 3). S100A7 was expressed predominantly in lymph node ERα$^-$ metastatic tumors. Its overexpression enhanced in vivo metastasis of ERα$^-$ cells. Furthermore, our studies suggest that S100A7 regulates breast cancer metastasis through a novel pathway by modulating actin cytoskeleton and MMP-9 activation. Since metastasis is the leading cause of cancer-related deaths, S100A7 could be a novel therapeutic target in ERα$^-$ metastatic breast cancer.

**Acknowledgments** This work was supported in part by grants from National Institutes of Health (CA109527 and CA153490) and Department of Defense to R.K. Ganju. Y.S. Deol was supported by Pelotonia Fellowship from Comprehensive Cancer Center, The Ohio State University. Authors thank Dr. Zahida Qamri, Dr. Nandu Thodi and Mohamed Adel for their help in in vivo BLI imaging. We also thank Viy McGaughy for IHC staining.

**Conflict of interest** None.

## References

1. Madsen P, Rasmussen HH, Leffers H, Honore B, Dejgaard K, Olsen E, Kiil J, Walbum E, Andersen AH, Basse B et al (1991) Molecular cloning, occurrence, and expression of a novel partially secreted protein "psoriasin" that is highly up-regulated in psoriatic skin. J Invest Dermatol 97(4):701–712

2. Schafer BW, Heizmann CW (1996) The S100 family of EF-hand calcium-binding proteins: functions and pathology. Trends Biochem Sci 21(4):134–140
3. Brodersen DE, Nyborg J, Kjeldgaard M (1999) Zinc-binding site of an S100 protein revealed. Two crystal structures of Ca2 + -bound human psoriasin (S100A7) in the $Zn^{2+}$-loaded and Zn2 + -free states. Biochemistry 38(6):1695–1704. doi:10.1021/bi982483d
4. Al-Haddad S, Zhang Z, Leygue E, Snell L, Huang A, Niu Y, Hiller-Hitchcock T, Hole K, Murphy LC, Watson PH (1999) Psoriasin (S100A7) expression and invasive breast cancer. Am J Pathol 155(6):2057–2066
5. Ji J, Zhao L, Wang X, Zhou C, Ding F, Su L, Zhang C, Mao X, Wu M, Liu Z (2004) Differential expression of S100 gene family in human esophageal squamous cell carcinoma. J Cancer Res Clin Oncol 130(8):480–486. doi:10.1007/s00432-004-0555-x
6. Wolf R, Ruzicka T, Yuspa SH (2010) Novel S100A7 (psoriasin)/S100A15 (koebnerisin) subfamily: highly homologous but distinct in regulation and function. Amino Acids 41(4):789–796. doi:10.1007/s00726-010-0666-4
7. Tripathi SC, Matta A, Kaur J, Grigull J, Chauhan SS, Thakar A, Shukla NK, Duggal R, DattaGupta S, Ralhan R, Siu KW (2010) Nuclear S100A7 is associated with poor prognosis in head and neck cancer. PLoS One 5(8):e11939. doi:10.1371/journal.pone.0011939
8. Emberley ED, Alowami S, Snell L, Murphy LC, Watson PH (2004) S100A7 (psoriasin) expression is associated with aggressive features and alteration of Jab1 in ductal carcinoma in situ of the breast. Breast Cancer Res 6(4):R308–R315 10.1186/bcr791
9. Emberley ED, Niu Y, Njue C, Kliewer EV, Murphy LC, Watson PH (2003) Psoriasin (S100A7) expression is associated with poor outcome in estrogen receptor-negative invasive breast cancer. Clin Cancer Res 9(7):2627–2631
10. Moog-Lutz C, Bouillet P, Regnier CH, Tomasetto C, Mattei MG, Chenard MP, Anglard P, Rio MC, Basset P (1995) Comparative expression of the psoriasin (S100A7) and S100C genes in breast carcinoma and co-localization to human chromosome 1q21-q22. Int J Cancer 63(2):297–303
11. Emberley ED, Murphy LC, Watson PH (2004) S100A7 and the progression of breast cancer. Breast Cancer Res 6(4):153–159. doi:10.1186/bcr816
12. Emberley ED, Niu Y, Leygue E, Tomes L, Gietz RD, Murphy LC, Watson PH (2003) Psoriasin interacts with Jab1 and influences breast cancer progression. Cancer Res 63(8):1954–1961
13. West NR, Watson PH (2010) S100A7 (psoriasin) is induced by the proinflammatory cytokines oncostatin-M and interleukin-6 in human breast cancer. Oncogene 29(14):2083–2092. doi:10.1038/onc.2009.488
14. Emberley ED, Niu Y, Curtis L, Troup S, Mandal SK, Myers JN, Gibson SB, Murphy LC, Watson PH (2005) The S100A7-c-Jun activation domain binding protein 1 pathway enhances prosurvival pathways in breast cancer. Cancer Res 65(13):5696–5702. doi:10.1158/0008-5472.CAN-04-3927
15. Paruchuri V, Prasad A, McHugh K, Bhat HK, Polyak K, Ganju RK (2008) S100A7-downregulation inhibits epidermal growth factor-induced signaling in breast cancer cells and blocks osteoclast formation. PLoS One 3(3):e1741. doi:10.1371/journal.pone.0001741
16. Deol YS, Nasser MW, Yu L, Zou X, Ganju RK (2011) Tumor-suppressive effects of psoriasin (S100A7) are mediated through the beta-catenin/T cell factor 4 protein pathway in estrogen receptor-positive breast cancer cells. J Biol Chem 286(52):44845–44854. doi:10.1074/jbc.M111.225466
17. Yu SE, Jang YK (2012) The histone demethylase LSD1 is required for estrogen-dependent S100A7 gene expression in human breast cancer cells. Biochem Biophys Res Commun 427(2):336–342. doi:10.1016/j.bbrc.2012.09.057
18. Burness ML, Grushko TA, Olopade OI (2010) Epidermal growth factor receptor in triple-negative and basal-like breast cancer: promising clinical target or only a marker? Cancer J 16(1):23–32. doi:10.1097/PPO.0b013e3181d24fc1
19. Eccles SA (2011) The epidermal growth factor receptor/Erb-B/HER family in normal and malignant breast biology. Int J Dev Biol 55(7–9):685–696. doi:10.1387/ijdb.113396se
20. Ridley AJ (2011) Life at the leading edge. Cell 145(7):1012–1022. doi:10.1016/j.cell.2011.06.010
21. Donaldson JG, Porat-Shliom N, Cohen LA (2009) Clathrin-independent endocytosis: a unique platform for cell signaling and PM remodeling. Cell Signal 21(1):1–6. doi:10.1016/j.cellsig.2008.06.020
22. Machacek M, Hodgson L, Welch C, Elliott H, Pertz O, Nalbant P, Abell A, Johnson GL, Hahn KM, Danuser G (2009) Coordination of Rho GTPase activities during cell protrusion. Nature 461(7260):99–103. doi:10.1038/nature08242
23. Nasser MW, Qamri Z, Deol YS, Ravi J, Powell CA, Trikha P, Schwendener RA, Bai XF, Shilo K, Zou X, Leone G, Wolf R, Yuspa SH, Ganju RK (2012) S100A7 enhances mammary tumorigenesis through upregulation of inflammatory pathways. Cancer Res 72(3):604–615. doi:10.1158/0008-5472.CAN-11-0669
24. Qamri Z, Preet A, Nasser MW, Bass CE, Leone G, Barsky SH, Ganju RK (2009) Synthetic cannabinoid receptor agonists inhibit tumor growth and metastasis of breast cancer. Mol Cancer Ther 8(11):3117–3129. doi:10.1158/1535-7163.MCT-09-0448
25. Minn AJ, Kang Y, Serganova I, Gupta GP, Giri DD, Doubrovin M, Ponomarev V, Gerald WL, Blasberg R, Massague J (2005) Distinct organ-specific metastatic potential of individual breast cancer cells and primary tumors. J Clin Invest 115(1):44–55. doi:10.1172/JCI22320
26. Dechow TN, Pedranzini L, Leitch A, Leslie K, Gerald WL, Linkov I, Bromberg JF (2004) Requirement of matrix metalloproteinase-9 for the transformation of human mammary epithelial cells by Stat3-C. Proc Natl Acad Sci USA 101(29):10602–10607. doi:10.1073/pnas.0404100101
27. Lin CC, Tseng HW, Hsieh HL, Lee CW, Wu CY, Cheng CY, Yang CM (2008) Tumor necrosis factor-alpha induces MMP-9 expression via p42/p44 MAPK, JNK, and nuclear factor-kappaB in A549 cells. Toxicol Appl Pharmacol 229(3):386–398. doi:10.1016/j.taap.2008.01.032
28. Delorme V, Machacek M, DerMardirossian C, Anderson KL, Wittmann T, Hanein D, Waterman-Storer C, Danuser G, Bokoch GM (2007) Cofilin activity downstream of Pak1 regulates cell protrusion efficiency by organizing lamellipodium and lamella actin networks. Dev Cell 13(5):646–662. doi:10.1016/j.devcel.2007.08.011
29. Arber S, Barbayannis FA, Hanser H, Schneider C, Stanyon CA, Bernard O, Caroni P (1998) Regulation of actin dynamics through phosphorylation of cofilin by LIM-kinase. Nature 393(6687):805–809. doi:10.1038/31729
30. Pollard TD, Borisy GG (2003) Cellular motility driven by assembly and disassembly of actin filaments. Cell 112(4):453–465
31. Guturi KK, Mandal T, Chatterjee A, Sarkar M, Bhattacharya S, Chatterjee U, Ghosh MK (2012) Mechanism of beta-catenin-mediated transcriptional regulation of epidermal growth factor receptor expression in glycogen synthase kinase 3 beta-inactivated prostate cancer cells. J Biol Chem 287(22):18287–18296. doi:10.1074/jbc.M111.324798
32. Duffy MJ, Maguire TM, Hill A, McDermott E, O'Higgins N (2000) Metalloproteinases: role in breast carcinogenesis, invasion and metastasis. Breast Cancer Res 2(4):252–257

33. Saleem M, Kweon MH, Johnson JJ, Adhami VM, Elcheva I, Khan N, Bin Hafeez B, Bhat KM, Sarfaraz S, Reagan-Shaw S, Spiegelman VS, Setaluri V, Mukhtar H (2006) S100A4 accelerates tumorigenesis and invasion of human prostate cancer through the transcriptional regulation of matrix metalloproteinase 9. Proc Natl Acad Sci USA 103(40):14825–14830. doi:10.1073/pnas.0606747103
34. Yong HY, Moon A (2007) Roles of calcium-binding proteins, S100A8 and S100A9, in invasive phenotype of human gastric cancer cells. Arch Pharm Res 30(1):75–81
35. Yamaguchi H, Condeelis J (2007) Regulation of the actin cytoskeleton in cancer cell migration and invasion. Biochim Biophys Acta 1773(5):642–652. doi:10.1016/j.bbamcr.2006.07.001
36. Wang W, Eddy R, Condeelis J (2007) The cofilin pathway in breast cancer invasion and metastasis. Nat Rev Cancer 7(6):429–440. doi:10.1038/nrc2148

Published OnlineFirst December 12, 2011; DOI: 10.1158/0008-5472.CAN-11-0669

Cancer Research

# S100A7 Enhances Mammary Tumorigenesis through Upregulation of Inflammatory Pathways

Mohd W. Nasser, Zahida Qamri, Yadwinder S. Deol, et al.

*Cancer Res* 2012;72:604-615. Published OnlineFirst December 12, 2011.

Cancer Research

# S100A7 Enhances Mammary Tumorigenesis through Upregulation of Inflammatory Pathways

Mohd W. Nasser[1], Zahida Qamri[1], Yadwinder S. Deol[1], Janani Ravi[1], Catherine A. Powell[1], Prashant Trikha[2], Reto A. Schwendener[3], Xue-Feng Bai[1], Konstantin Shilo[1], Xianghong Zou[1], Gustavo Leone[2], Ronald Wolf[4], Stuart H. Yuspa[5], and Ramesh K. Ganju[1]

## Abstract

S100A7/psoriasin, a member of the epidermal differentiation complex, is widely overexpressed in invasive estrogen receptor (ER)α-negative breast cancers. However, it has not been established whether S100A7 contributes to breast cancer growth or metastasis. Here, we report the consequences of its expression on inflammatory pathways that impact breast cancer growth. Overexpression of human S100A7 or its murine homologue mS100a7a15 enhanced cell proliferation and upregulated various proinflammatory molecules in ERα-negative breast cancer cells. To examine *in vivo* effects, we generated mice with an inducible form of mS100a7a15 (MMTV-mS100a7a15 mice). Orthotopic implantation of MVT-1 breast tumor cells into the mammary glands of these mice enhanced tumor growth and metastasis. Compared with uninduced transgenic control mice, the mammary glands of mice where mS100a7a15 was induced exhibited increased ductal hyperplasia and expression of molecules involved in proliferation, signaling, tissue remodeling, and macrophage recruitment. Furthermore, tumors and lung tissues obtained from these mice showed further increases in prometastatic gene expression and recruitment of tumor-associated macrophages (TAM). Notably, *in vivo* depletion of TAM inhibited the effects of mS100a7a15 induction on tumor growth and angiogenesis. Furthermore, introduction of soluble hS100A7 or mS100a7a15 enhanced chemotaxis of macrophages via activation of RAGE receptors. In summary, our work used a powerful new model system to show that S100A7 enhances breast tumor growth and metastasis by activating proinflammatory and metastatic pathways. *Cancer Res; 72(3); 604–15. ©2011 AACR.*

## Introduction

Human S100A7 (hS100A7) is present within the epidermal differentiation complex on 1q21 chromosome (1) and is predominantly expressed in high-grade ductal carcinoma *in situ* (DCIS; refs. 2–6). In addition, its expression is significantly associated with estrogen receptor (ER)α-negative and nodal metastasis in invasive ductal tumors (2, 4–6). Furthermore, hS100A7 expression is associated with increased angiogenesis (7). hS100A7 has been shown to modulate tumor growth by activating several signaling pathways (5, 8–10).

**Authors' Affiliations:** [1]Department of Pathology; [2]Molecular Cancer Genetics, The Ohio State University, Columbus, Ohio; [3]Institute of Molecular Cancer Research, University of Zurich, Zurich, Switzerland; [4]Department of Dermatology and Allergology, Ludwig Maximilian University, Munich, Germany; and [5]Laboratory of Cancer Biology and Genetics, National Cancer Institute, Bethesda, Maryland

**Note:** Supplementary data for this article are available at Cancer Research Online (http://cancerres.aacrjournals.org/).

**Corresponding Author:** Ramesh K. Ganju, Department of Pathology, Ohio State University, 185 Hamilton Hall, 1645 Neil Ave, Columbus, OH 43210. Phone: 614-292-5539; Fax: 614-292-7072; E-mail: Ramesh.Ganju@osumc.edu

**doi:** 10.1158/0008-5472.CAN-11-0669



hS100A7 has also been associated with increased inflammatory cell infiltrates in invasive breast tumors (2) and various inflammatory disorders (2). Cytokines, including oncostatin M (OSM), interleukin (IL)-6, and IL-1, have been shown to induce hS100A7 (10). These cytokines directly or indirectly signal through STAT3 pathways (11, 12). STAT3 has been shown to be constitutively activated in 35% to 60% of human breast cancers (13). Activated STAT3 has also been shown to be associated with increased expression of cytokines, growth factors, matrix metalloproteinases (MMP), and angiogenic factors (12). In addition, STAT3 signaling modulates tumor growth and metastasis by recruitment of tumor-associated macrophages (TAM) to tumors (14, 15). TAMs, which often constitute a major part of leukocyte infiltrates present in the tumor microenvironment, have been shown to enhance the tumor growth and metastasis of various cancers (16, 17). In addition, collaborative interactions of tumors with TAMs have been associated with poor prognosis in breast cancer (16, 18). Studies with mouse models have shown that ablation of macrophages leads to inhibition of tumor progression and metastasis (19–21). Factors produced by tumor cells, especially cytokines/chemokines, activate TAMs, which in turn release factors that stimulate tumor cell proliferation, angiogenesis, and metastasis (17, 20).

Transgenic mouse models of human breast cancer have provided important information about the initiation and progression of breast cancer and thus have emerged as powerful

tools for preclinical research. Phylogenetic analyses have shown the mouse ancestor mS100a7a15 to be most related to S100A7 and S100A15 among the human paralogs (22, 23). mS100a7a15 has been shown to be upregulated in carcinogen-induced mammary tumorigenesis (22). However, the direct functional role of mS100a7a15 in disease progression is not well characterized. In this study, we have generated a novel transgenic mouse model MMTV-rtTA; tetO-mS100a7a15 (MMTV-mS100a7a15) to study the functional significance of mS100a7a15 in breast tumorigenesis. We have used this model to analyze the role of mS100a7a15 in breast cancer growth/metastasis and have shown that mS100a7a15 may enhance tumorigenesis by inducing proinflammatory molecules and recruiting TAMs.

## Materials and Methods

### Cell culture and transfection

Human breast carcinoma cell line MDA-MB-231 (American Type Culture Collection) and MVT-1 cells derived from MMTV-c-Myc; MMTV-VEGF bitransgenic mice (obtained from Dr. Johnson) were cultured (24, 25). The identity of these cell lines was regularly verified on the basis of cell morphology. cDNA of hS100A7 (OriGene Technologies) and cDNA of mS100a7a15 were subcloned into pIRES2-EGFP (Invitrogen). Cells were transfected with pIRES2-EGFP-hS100A7 or pIRES2-EGFP-mS100a7a15 or pIRES-2-EGFP using Lipofectamine reagent according to the manufacturer's instructions and stable clones were generated using G418 (500 μg/mL).

### Cell proliferation

Cell proliferation of hS100A7 or mS100a7a15 overexpressing or vector expressing MDA-MB-231 cells was determined as described (24).

### Chemotaxis

The chemotactic assays were carried out using Transwell chambers (Costar 8 μm pore size; ref. 24). Briefly, phorbol-12-myristate 13-acetate (100 ng/mL) THP1-differentiated macrophages (TDM) or murine macrophage RAW264.7 cells (MMR) were serum starved. Top chambers were loaded with 150 μL of $1 \times 10^6$ cells/mL in serum-free medium (SFM) and bottom chambers had 600 μL of SFM containing 50 μg of concentrated supernatant obtained from hS100A7- or mS100a7a15-overexpressing or vector-expressing MDA-MB-231 cells. Migrated cells were fixed and documented as described (24).

### Western blot analysis

Western blot analysis of lysates was done as described (24).

### Microarray analysis

Total RNA was collected from hS100A7-overexpressing or vector expressing MDA-MB-231 cells using TRIzol reagent (Invitrogen). Microarray analysis was done at the Ohio State University (Columbus, OH) core facility using an Affymetrix Microarray gene U133 chip containing 40,000 human genes. The data were deposited in the GEO Expression Omnibus under accession no. GSE32052 (Supplementary Table S1).

### Generation of transgenic mice

TetO-mS100a7a15 mice (26) were cross-bred with MMTV-rtTA mice (provided by Dr. Chodosh) to generate bitransgenic MMTV-mS100a7a15 mice. Transgenic littermates were genotyped by PCR using tetO-mS100a7a15 primers (Supplementary Table S1). Female mice were fed with Dox-chow 1 g/kg (Harlan laboratories) and mice fed with normal diet served as controls. All transgenic mice were kept in animal facility of Ohio State University in compliance with the guidelines and protocols approved by the IACUC.

### Whole mount analysis of mammary glands

Right inguinal mammary gland #4 were spread on glass slides, fixed and stained overnight with 0.2% (w/v) carmine (Sigma) and 0.5% (w/v) aluminum sulfate (Sigma) as described (27).

### Orthotopic injection assay

A total of $1 \times 10^5$/100 μL of murine MVT-1 cells were injected into mammary gland (#4) of transgenic mice. Injected mice were either fed with Dox-chow 1 g/kg for 28 days or normal diet (control). Tumors were measured weekly with external calipers, and volume was calculated according to the formula $V = 0.52 \times a^2 \times b$, where $a$ is the smallest superficial diameter and $b$ is the largest superficial diameter. Orthotopically injected animals were sacrificed 28 days postinjection and tumors were excised and processed (28).

### Depletion of macrophages using clodronate liposomes

Clodronate liposomes (clodrolip) were prepared as described (21). Briefly, clodrolip (1.5 mg/kg) was injected intraperitoneally 6 hours after tumor cell implantation and followed by 0.75 mg/kg treatments every 4 days. Control groups received PBS-liposomes at the same time points. The mice were sacrificed 25 days postinjection and tumors were excised and processed.

### FACS analysis

For fluorescence-activated cell-sorting (FACS) analysis, freshly prepared single-cell suspension of tumor-infiltrating cells was incubated with anti-F4/80 PE, anti-Cd11b APC, and anti-CD206 Alexa Flour 488 (29). Receptor for advanced glycation end products (RAGE) expression was analyzed by staining with RAGE antibody (Abcam) followed by Alexa Flour 488 antibody. After staining, the cells were analyzed by FACS Caliber using CellQuest software (BD Biosciences).

### Immunohistochemistry

Samples from mammary gland and tumors were dissected, fixed in formalin and embedded in paraffin for sections. Standard immunohistochemical techniques were used according to the manufacturer's recommendations (Vector Laboratories) using antibodies against Ki67 (Neomarkers, 1:100), CD31 (Santa Cruz 1:100), Keratin-8 (Troma-1 1:100), mS100a7a15 (custom, 1:250), F4/80 (AbD Serotec, 1:50), arginase1 (Santa Cruz, 1:200), and rabbit anti-mouse inducible nitric oxide synthase (iNOS; Abcam, 1:200) for 60 minutes at room temperature. Vectastain Elite ABC reagents (Vector

Laboratories), using avidin DH:biotinylated horseradish peroxidase H complex with 3,3′-diaminobenzidine (Polysciences) and Mayer's hematoxylin (Fisher Scientific), were used for detection of the bound antibodies.

### Reverse transcriptase and real-time PCR

RNA was isolated from cells, mouse mammary gland, and tissues using TRIzol reagent (Invitrogen). Reverse transcriptase PCR (RT-PCR) reaction was carried out using RT-PCR kits (Applied Biosystem). Expression of genes analyzed by quantitative PCR (qPCR) was normalized to glyceraldehyde-3-phosphate dehydrogenase (GAPDH) or 18SRNA using the $2^{(-\Delta C_t)}$ method (30). Primers used for RT-PCR and qPCR are listed in Supplementary Table S1.

### Statistical analysis

Student *t* test was used to compare different experimental groups. $P < 0.05$ was considered to be statistically significant. For all graphs, $^{*}$, $P < 0.05$; $^{**}$, $P < 0.01$.

## Results

### hS100A7 and mS100a7a15 overexpression induce proliferation and expression of inflammatory cytokines/chemokines

hS100A7 has been shown to be highly associated with ERα$^{-}$ breast cancers. Therefore, we first analyzed the effect of hS100A7 overexpression on proliferation of the ERα$^{-}$ MDA-MB-231 cell line using 2 different clones, S1 and S2. hS100A7 expression was confirmed by Western blot (Fig. 1A, left). hS100A7 overexpression significantly enhanced growth in both the clones, compared with vector control (V; Fig. 1A, right). To determine the mechanism by which hS100A7 may enhance tumorigenesis, we carried out microarray analysis and found that hS100A7 overexpression induced high levels of proinflammatory cytokines/chemokines CXCL1, CXCL8, IL-1α, IL-11, and CSF2 as compared with control (Fig. 1B). The expression of these hS100A7-induced target proteins was further confirmed using qPCR in 2 different clones, S1 and S2 (Fig. 1C).

Phylogenetic analyses have shown that mS100a7a15 is most related to hS100A7 and hS100A15 (22, 23). mS100a7a15 has also been shown to be associated with inflammation (31). Similar to hS100A7, mS100a7a15 overexpression in 2 different clones of MDA-MB-231 (M1 and M2) enhanced proliferation (Fig. 1D, bottom) and expression of inflammatory molecules CXCL1, CXCL8, IL-1α, IL-11, and CSF2 as compared with vector (Fig. 1E). These results suggest that hS100A7 and mS100a7a15 overexpression enhance growth and upregulate proinflammatory cytokine/chemokine production in breast cancer cells.

### mS100a7a15 induces mammary hyperplasia in bitransgenic mice

It has been reported that mS100a7a15 is upregulated during carcinogen-induced mammary tumorigenesis (22). However, to the best of our knowledge, there is no transgenic/knockout mouse model available to study the role of mS100a7a15 in breast tumorigenesis. Very recently, K5-tTA; tetO-mS100a7a15 mice were generated for studying the role of mS100a7a15 in psoriasis (26). To determine the role of mS100a7a15 in tumorigenesis, we generated an inducible transgenic mouse model by crossing tetO-mS100a7a15 mice with tetracycline-responsive transactivator protein under the murine mammary tumor virus (MMTV-rtTA) promoter mice. In the presence of doxycycline, rtTA protein changes its conformation and binds to *tet* operator (tet-O) sequences that result in expression of mS100a7a15 in mammary epithelial cells (Fig. 2A). The mice were genotyped with mS100a7a15 and MMTV-rtTA–specific primers (data not shown). Mammary gland derived from MMTV-mS100a7a15 mice that were subjected to Dox-chow (1 g/kg) for 3 months showed mS100a7a15 expression at mRNA levels (Fig. 2B, left). We also observed enhanced mS100a7a15 expression in these mice by immunohistochemistry (IHC; Fig. 2B, right). We further identified the mS100a7a15-overexpressing cells to be of luminal epithelial origin as these cells also express CK8 (Fig. 2B, right). Further morphologic examination of whole mount virgin mammary gland by carmine (Fig. 2C, top) or hematoxylin and eosin (H&E; Fig. 2C, bottom) staining showed ductal hyperplasia in the doxycycline-induced MMTV-mS100a7a15 mice compared with uninduced mice. These findings indicate that overexpression of mS100a7a15 in mouse mammary gland induces hyperplasia.

### mS100a7a15 overexpression in mammary glands enhances proliferative, inflammatory, and signaling pathways

We analyzed the expression of phospho-STAT3, phospho-AKT, phospho-ERK, and cyclin D1 in mammary gland as these molecules have been shown to be associated with proinflammatory and proliferative responses and are activated in breast cancer tissue (12, 13, 32). We observed enhanced phosphorylation of STAT3, ERK, and AKT in doxycycline-treated MMTV-mS100a7a15 mice (Fig. 2D). We also observed enhanced expression of cyclin D1 by Western blot (Fig. 2D) and expression of Ki67 and cyclin D1 by IHC (Fig. 2E) in doxycycline-induced MMTV-mS100a7a15 mice. Because STAT3 has been shown to enhance macrophage infiltrations to the tumors (12), we further analyzed the recruitment of macrophages in the mammary gland of these mice. We found an increase in macrophages in doxycycline-induced MMTV-mS100a7a15 compared with uninduced mice (Fig. 2E). MMPs are known to degrade extracellular matrix (ECM) proteins in the cellular microenvironment and significant correlation between TAM count and MMP expression has been observed in tumor (33–35). We observed enhanced MMP2 expression in the mammary gland of doxycycline-induced MMTV-mS100a7a15 compared with uninduced mice (Fig. 2D). These data indicate that mS100a7a15 overexpression induces hyperplasia, activates STAT3/AKT/ERK pathways, and enhances the macrophage recruitment.

### mS100a7a15 enhances tumor growth in an orthotopic syngeneic breast cancer model

hS100A7 has been shown to increase tumor growth in nude mice (5, 7). We further analyzed the role of mS100a7a15 in tumor progression, by implanting highly aggressive MVT-1 cells (25) into the mammary gland of MMTV-mS100a7a15 mice. Five days prior to injection, mice ($n = 5$) were fed with

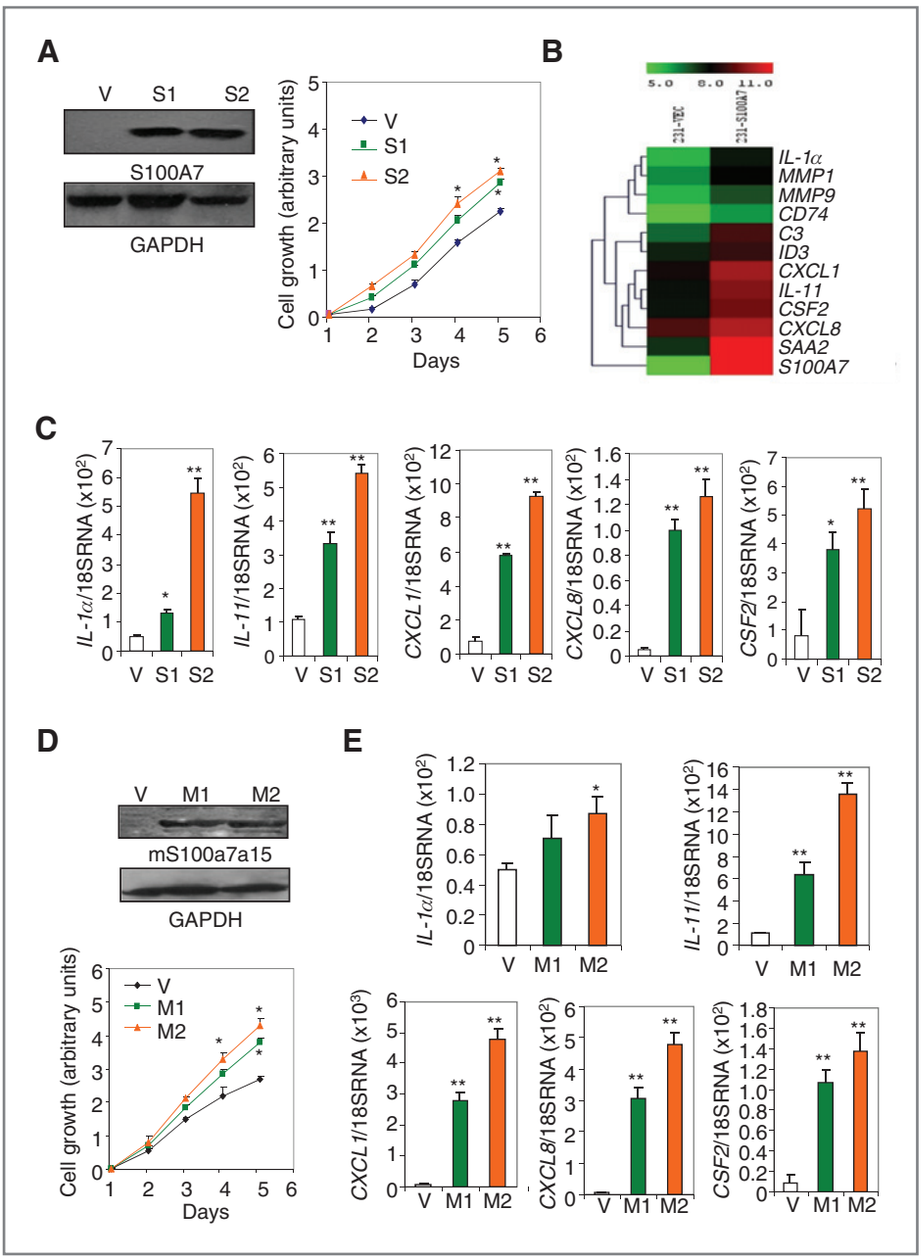


**Figure 1.** Effect of hS100A7 and mS100a7a15 overexpression on proliferation and proinflammatory gene expression. A, left, the expression of hS100A7 in 2 different clones of MDA-MB-231 cells (S1 and S2) was analyzed by Western blot using hS100A7-specific antibody. GAPDH was used as the loading control. A, right, proliferation of hS100A7-expressing MDA-MB-231 (S1 and S2) and vector control cells (V) was analyzed using MTT assay. B, heatmap of differentially expressed genes in MDA-MB-231–overexpressing hS100A7 (231-S100A7) compared with control (231-Vec). C, expression of transcripts for indicated inflammatory markers relative to 18SRNA in vector or hS100A7-overexpressing cells (S1 and S2) by qPCR. D, top, the expression of mS100a7a15 in 2 different clones of MDA-MB-231 cells (M1 and M2) was analyzed by Western blot using mS100a7a15 antibody. D, bottom, proliferation of mS100a7a15-expressing MDA-MB-231 (M1 and M2) and vector cells was analyzed using the MTT assay. E, expression of transcripts of inflammatory markers as analyzed by qPCR in mS100a7a15 overexpressing clones M1 and M2. All the experiments were repeated 3 times and representative ones are shown. Graphs represent the mean ± SD for each experimental group. *, $P < 0.05$; **, $P < 0.01$.

1 g/kg Dox-chow to induce mS100a7a15 and mice maintained on normal diet served as control. These mice were observed for tumor growth (Fig. 3A, left). Interestingly, MVT-1–derived tumor growth was enhanced 2-fold in doxycycline-treated MMTV-mS100a7a15 compared with the uninduced mice (Fig. 3A, middle and right). These studies show that mS100a7a15 expression in mammary gland enhanced growth of breast cancer cells in syngeneic mouse models.

### mS100a7a15 overexpression enhances TAM recruitment in a syngeneic mouse model

TAMs have been shown to be a major component of inflammatory infiltrates seen in tumors (18, 20). Initially, MVT-1–derived primary tumors were evaluated by IHC with macrophage marker F4/80. F4/80$^+$ macrophages were enhanced in tumor tissues of doxycycline-induced MMTV-mS100a7a15 compared with uninduced mice (Fig. 3B). We further analyzed macrophage infiltration in the tumors by flow cytometry. As shown in Fig. 3C, the CD11b$^+$/F4/80$^+$ macrophage infiltration was increased by approximately 42% in doxycycline-induced MMTV-mS100a7a15 compared with uninduced mice. We also analyzed other cell types such as Gr-1, T, and B cells but did not notice any significant increase in the doxycycline-induced MMTV-mS100a7a15 compared with uninduced mice (data not shown).

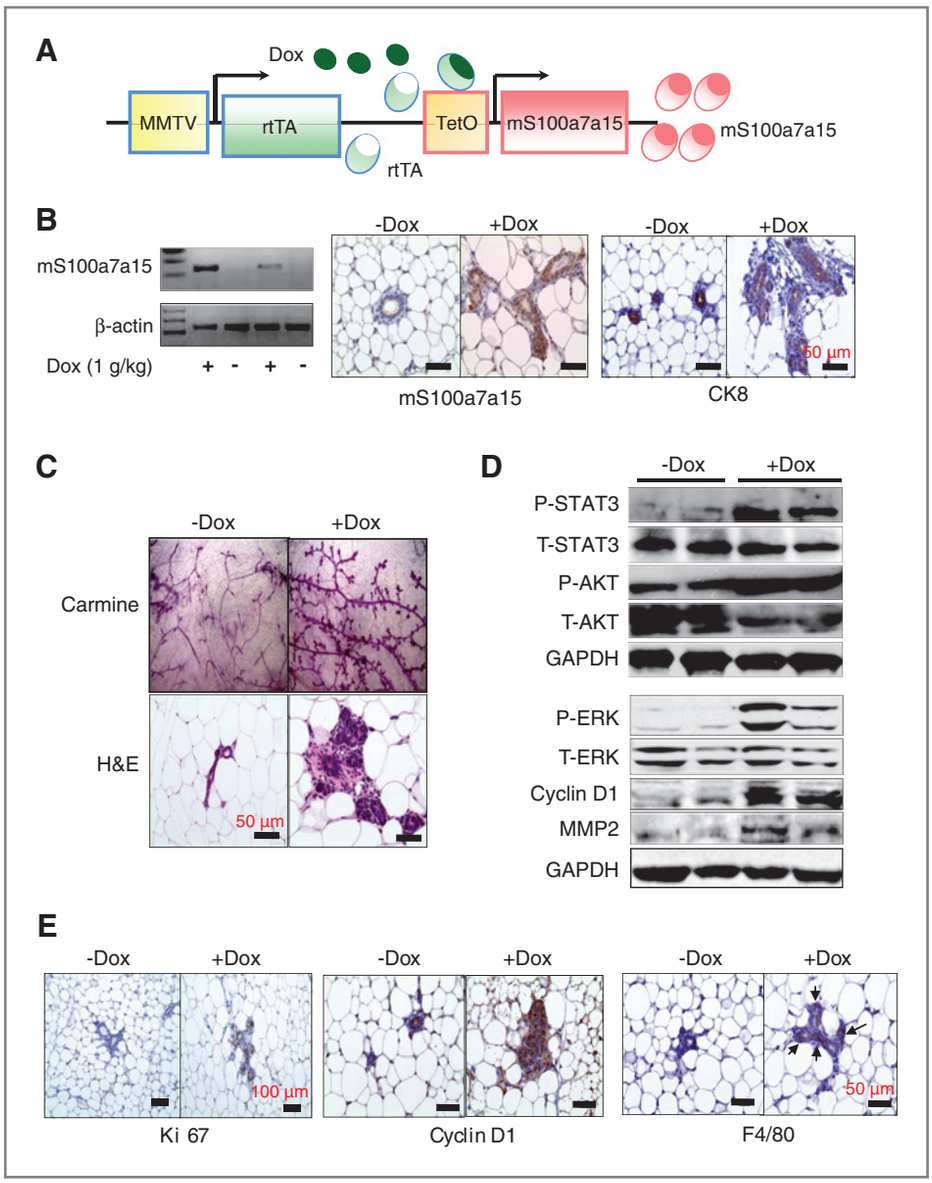


**Figure 2.** Characterization of the inducible, mammary-specific mS100a7a15 transgenic mouse model. A, schematic representation of the inducible, MMTV-mS100a7a15 (Tet-O, tet operator) mouse model system. B, left, RT-PCR analysis of mS100a7a15 expression in mammary gland of doxycycline-induced and uninduced mice ($n = 5$). B, right, immunohistochemical analysis of mS100a7a15 and CK8 of mammary gland from doxycycline-treated (+Dox) and untreated (−Dox) mice. C, top, mammary gland from doxycycline-treated (+Dox) and untreated (−Dox) mice were subjected to whole mount carmine staining (Original magnification of 40×) or (C, bottom) H&E staining. D, mammary gland lysates (50 μg) from MMTV-mS100a7a15 mice treated with doxycycline or untreated were subjected to Western blot using phospho-STAT3, phospho-ERK, phospho-AKT (P-STAT3, P-ERK, P-AKT), cyclin D1, and MMP2 antibodies. Blot showing anti-GAPDH indicates equal loading of lysates. E, mammary gland isolated from doxycycline-treated and untreated ($n = 5$) mice were subjected to IHC of Ki67, cyclin D1, and F4/80. Representative photomicrographs of 5 mammary tissues per experimental group.

TAMs can be divided into 2 main classes, tumor-suppressive M1 (classically activated) and tumor-promoting M2 (alternative). M1 macrophages are characterized among other factors by expression of iNOS whereas M2 macrophages have a decreased level of iNOS and are identified by their signature expression of arginase-1 (Arg-1) and mannose receptor (CD206; ref. 36). An increase of 29% $CD11b^+$/CD206 (M2 TAM) was observed in tumors derived from doxycycline-induced MMTV-mS100a7a15 compared with uninduced mice (Fig. 3D). We further confirmed increased M2 phenotype by IHC for enhanced expression of Arg-1 and decreased iNOS expression (Fig. 3E, left). Changes in expression of *Arg-1* or *iNOS* genes were also detected by qPCR (Fig. 3E, right). These results suggest that mS100a7a15 may enhance tumor growth by recruiting M2 macrophages to the tumor site.

### mS100a7a15 overexpression induces the expression of metastatic and angiogenic markers

We examined the expression of prometastatic and angiogenic genes, such as *CCL2*, *COX2*, *MMP9*, and *VEGF*, in the MVT-1–derived tumors. These genes were significantly upregulated in doxycycline-induced MMTV-mS100a7a15 compared with uninduced mice (Fig. 4A and B). We also observed an approximately 2.7-fold increase in $CD31^+$ blood vessels as detected by IHC in doxycycline-induced MMTV-mS100a7a15 compared with uninduced mice (Fig. 4C and D). These studies suggest that mS100a7a15

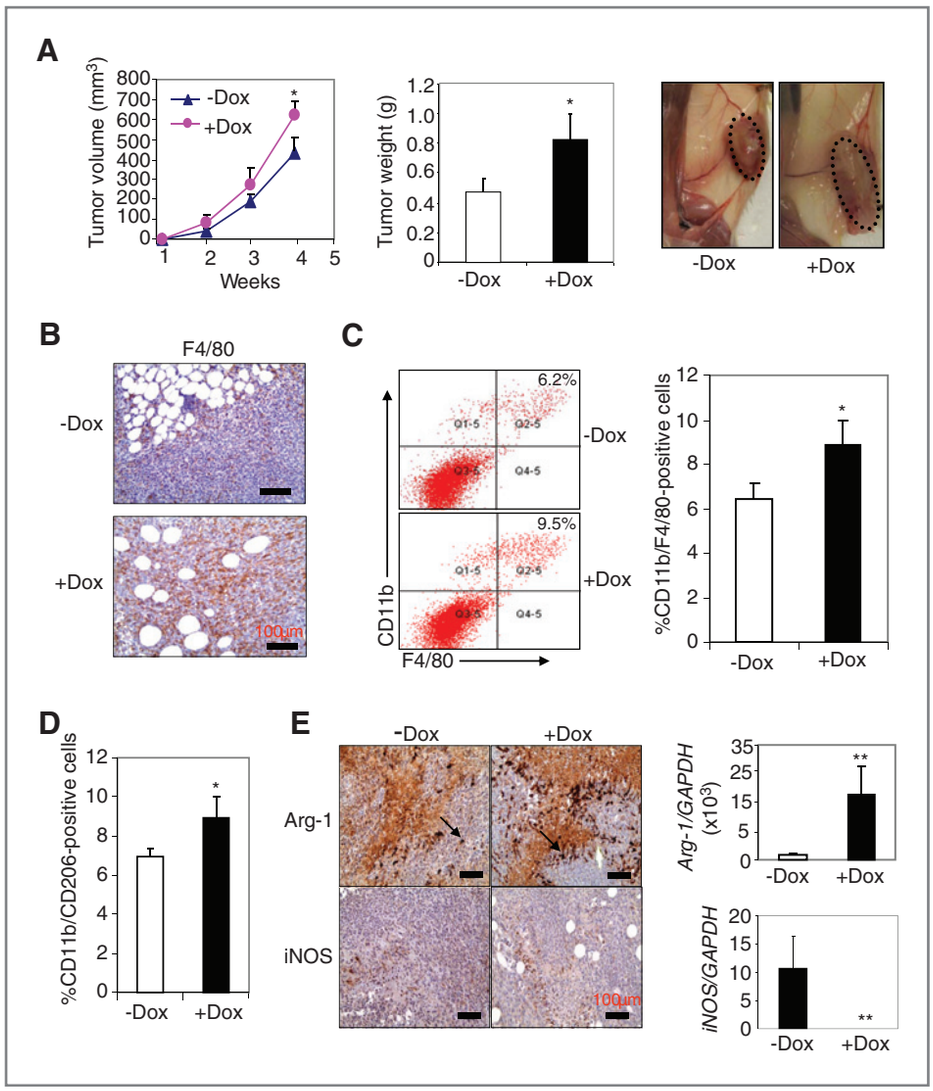


**Figure 3.** Effect of mS100a7a15 on tumor growth in orthotopic syngeneic model. A, left, MVT-1 cells were injected into the mammary gland of the MMTV-mS100a7a15 mice ($n = 5$) and tumor volume was measured every week. A, middle, after 28 days, the tumors were excised from mice and weighed. A, right, representative photograph of mice showing tumors dissected from different experimental groups. B, MVT-1 cell line derived tumors from doxycycline-treated and untreated MMTV-mS100a7a15 mice were subjected to immunohistochemical staining for macrophage marker, F4/80. (C) $CD11b^+F4/80^+$ cells and (D) $CD11b^+CD206^+$ were quantified by flow cytometry in disaggregated MVT1 primary tumors harvested 28 days after implantation from doxycycline-treated and untreated MMTV-mS100a7a15 mice. E, right, IHC of Arginase-1 (Arg-1) and iNOS. E, left, expression of *Arg-1* and *iNOS* by qPCR. Data represent the mean ± SD of 3 independent experiments. *, $P < 0.05$; **, $P < 0.01$.

may enhance expression of metastatic and angiogenic markers.

### mS100a7a15 overexpression enhances metastasis in orthotopic breast cancer models

We further investigated the role of mS100a7a15 on spontaneous metastasis in MMTV-mS100a7a15 mice injected with MVT-1 cells. We observed a significant increase in surface lung metastases in the mice treated with doxycycline compared with untreated mice ($P < 0.049$; Fig. 5A and B). Because TAMs have been shown to enhance metastasis (17, 18, 20), we further analyzed the infiltrations of macrophages in the lung tissues and observed enhanced expression of $F4/80^+$ macrophages (Fig. 5C) and Arg-1 expression but decreased iNOS expression (Fig. 5C) in doxycycline-induced MMTV-mS100a7a15 compared with untreated mice. We also observed a significant increase in prometastatic genes, such as *CCL2* and *VEGF*, in the metastatic lung tissue of doxycycline-induced MMTV-mS100a7a15 compared with uninduced mice (Fig. 5D). These studies suggest that mS100a7a15 may enhance metastasis through enhancement of prometastatic genes in the metastatic lungs.

### Macrophage depletion inhibits tumor growth and angiogenesis

To specifically analyze the role of mS100a7a15 overexpression in TAM recruitment, we selectively inhibited macrophages using clodrolip (liposome-encapsulated clodronate) as previously described (21). Clodrolip treatment significantly reduced tumor growth in MVT-1–derived doxycycline-induced MMTV-mS100a7a15 compared with control liposome–treated mice (Fig. 6A and B). Quantification of the number of $F4/80^+$ TAMs and $CD206^+$ M2 TAMs by FACS (Fig. 6C) and IHC (Fig. 6D and E left) revealed a significant decrease in TAMs and M2 TAMs in clodrolip treated compared with control liposome–treated mice fed with doxycycline diet. We also observed significant reduction in angiogenesis as detected by $CD31^+$ immunohistochemical staining in clodrolip-treated MMTV-

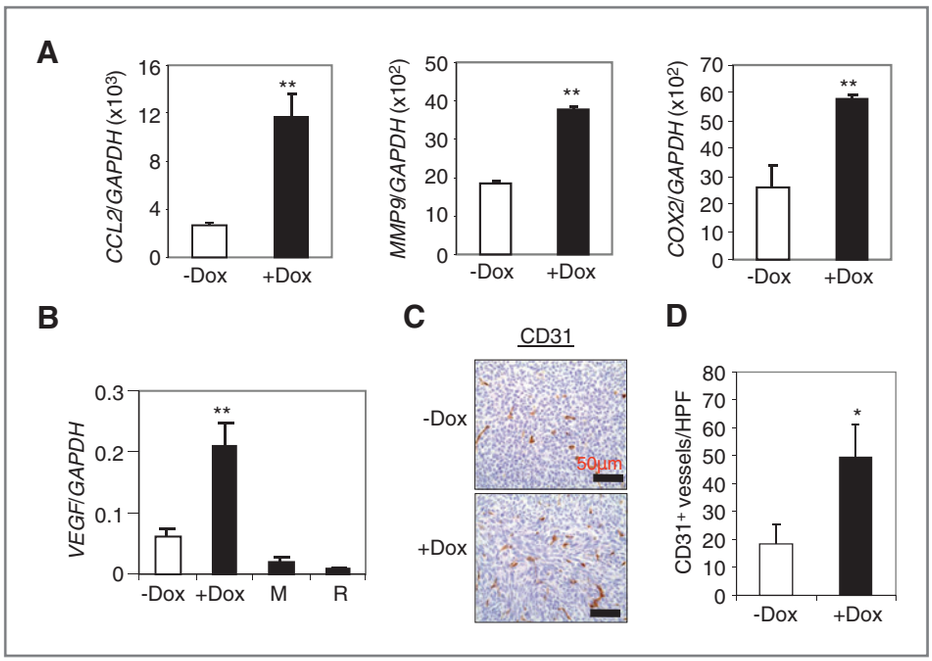


**Figure 4.** Effect of mS100a7a15 expression on prometastatic and angiogenic markers. A, gene expression was quantified by qPCR in mammary tumors from doxycycline-treated and untreated MMTV-mS100a7a15 mice ($n = 5$). B, *VEGF* expression in doxycycline-treated and untreated MMTV-mS100a7a15 mice and MVT-1 (M) or RAW264.7 (R) cell lines. C, representative IHC with endothelial marker CD31 antibody to assess the number of blood vessels in tumors from doxycycline-treated compared with untreated mice. D, bars represent the mean ± SD of the number of $CD31^+$ blood vessels shown in (C) counted in 5 random high-power fields (HPF, 20×) per tissue section ($n = 5$). *, $P < 0.05$; **, $P < 0.01$.

mS100a7a15 compared with control liposome–treated mice fed with doxycycline diet (Fig. 6D, bottom, and 6E, right). These studies further confirm that mS100a7a15 may enhance tumorigenesis and angiogenesis through recruitment of macrophages.

### Soluble hS100A7 and mS100a7a15 enhance chemotaxis in macrophages *in vitro*

Previously, soluble hS100A7 and mS100a7a15 were shown to induce chemotaxis in leukocytes by binding to RAGE (26, 37). However, not much is known about the role of these proteins in regulating monocyte/macrophage chemotaxis. We analyzed the effect of hS100A7 secreted into the conditioned media on chemotaxis of the differentiated monocytic cell line THP-1. hS100A7 expression was observed in the supernatant of hS100A7-overexpressing MDA-MB-231 cells (Fig. 7A, left). We also observed expression of RAGE in TDM (Fig. 7A, right). Furthermore, we observed a significant increase in the chemotaxis of TDM upon stimulation with conditioned media of hS100A7-MDA-MB-231 cells. These effects were significantly abrogated by blocking RAGE (Fig. 7B). We have also shown that RAGE is expressed on the surface of MMR (Fig. 7C). We also observed mS100a7a15 expression in the conditioned media of mS100a7a15-overexpressing MDA-MB-231 cells (Fig. 7C, right). In addition, conditioned media of mS100a7a15-expressing MDA-MB-231 cells enhanced migration of MMR and these effects were blocked by murine RAGE–neutralizing antibodies (Fig. 7D). These studies suggest that hS100A7/mS100a7a15 may enhance monocyte/macrophage chemotaxis through RAGE.

## Discussion

hS100A7 has been shown to be associated with the $ER\alpha^-$ phenotype and is predominantly expressed in high-grade DCIS. Furthermore, expression of hS100A7 in breast tumors represents a poor prognostic marker and correlates with lymphocyte infiltration and high-grade morphology (2, 6, 7). Although a number of putative functions have been proposed for hS100A7, its biologic role particularly in breast cancer remains to be defined.

In this study, we characterized the tumor-enhancing effects of hS100A7 and mS100a7a15 in MDA-MB-231 breast cancer cells and inducible MMTV-mS100a7a15 mouse model systems. We observed enhanced proliferation and production of proinflammatory molecules IL-1α, IL-11, CSF2, CXCL1, and CXCL8 in hS100A7 and mS100a7a15-overexpressing cells compared with vector control. These molecules have been shown to play a major role in tumor progression and invasion (38, 39).

In an inducible transgenic mouse model system, we observed a significant increase in the number of primary ducts and side branches in mice expressing mS100a7a15 in mammary epithelial cells. This increase in mammary ductal epithelial hyperplasia was caused by enhanced proliferation as indicated by increased expression of Ki67 and cyclin D1 in the ductal epithelial cells of induced mice. We observed increased expression of STAT3 and MMP2 in mammary gland of inducible mice. Overexpression of cyclin D1 has been reported in up to 50% of primary breast tumors (40). In addition, STAT3 has been shown to be constitutively activated in 35% to 60% of breast cancers (12).

We also showed that mS100a7a15 overexpression significantly increased tumor growth in the syngeneic orthotopic model. Further elucidation of mechanisms revealed that mS100a7a15 may enhance growth and metastasis through recruitment of M2 TAMs. M2-polarized TAMs are known to drive tumor progression by stimulating angiogenesis and metastasis (17, 18, 20). We have shown that M2-specific markers are increased whereas expression of M1 markers is

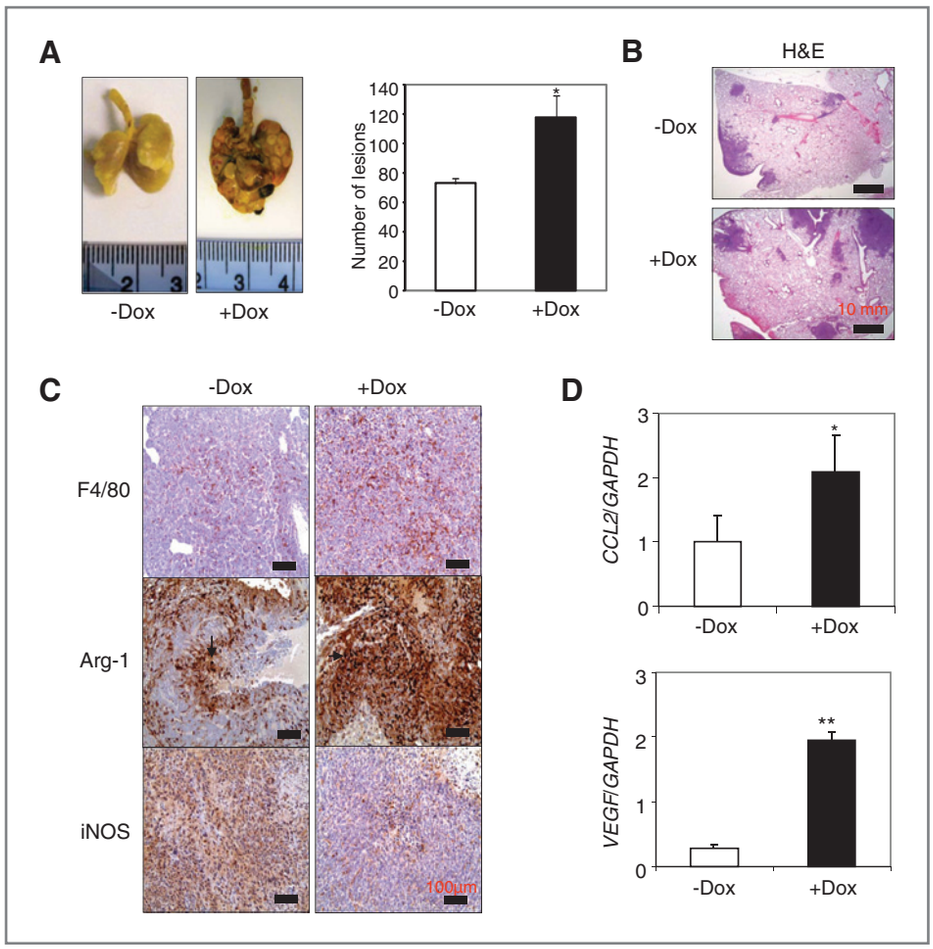


**Figure 5.** Effect of mS100a7a15 on metastasis and TAM infiltrations. MVT-1 cells were injected into the mammary gland of the inducible MMTV-mS100a7a15 mice. A, left, representative photographs of metastatic nodules in the lung of doxycycline-treated ($n = 4$) and untreated ($n = 5$) mice. A, right, lungs were removed and inflated with Bouin's fixative, and the number of metastatic nodules on the lungs was counted with the aid of a dissecting microscope (29). B, H&E staining of metastatic nodules in the lung of doxycycline-treated MMTV-mS100a7a15 or untreated mice. C, IHC of F4/80, Arg-1, and iNOS in metastatic lung tissues obtained from doxycycline-treated and untreated MMTV-mS100a7a15 mice. D, expression of *CCL2* and *VEGF* by qPCR. Data represent the mean ± SD per experimental group. *, $P < 0.05$; **, $P < 0.01$.

decreased in MVT-1–derived tumors and lung tissues of doxycycline-induced mS100a7a15 mice. We further determined whether selective depletion of macrophages would inhibit tumor growth. It has been shown previously that macrophages may be selectively depleted in mice using clodrolip (21). Therefore, we treated MVT-1 tumor–bearing mice with intraperitoneal inoculations of clodrolip or with an empty liposome control at various points throughout tumor progression. We observed approximately 80% depletion of macrophage content of the tumors compared with control liposome–treated tumors in doxycycline-induced MMTV-S100a7a15 mice. We observed that clodrolip-mediated reduction of TAMs also caused dramatic reduction in tumor growth in doxycycline-induced MMTV-mS100a7a15 mice. These results suggest that mS100a7a15 may enhance tumor growth through enhancing recruitment of macrophages to the tumors. Previous studies have reported that an intimate relationship between macrophages and tumor cells is required for tumor growth and metastasis (18, 41). We have shown that hS100A7 and mS100a7a15 enhanced chemotaxis of monocyte/macrophages through RAGE. RAGE expression has been detected in a variety of human tumors including breast (42). It has been shown that the blockade of RAGE in glioma-suppressed tumor growth (43).

Although mS100a7a15 has been shown to enhance CD4-positive T-cell populations in mS100a7a15-overexpressing keratinocytes from psoriasis mouse model (26), we did not observe a significant change in CD4-positive T cells as detected by FACS in tumors derived from our MVT-1 orthotopic syngeneic model. This difference may be attributed to the different model systems used in each study. Another possibility is that the recruitment of macrophages could result from enhanced production of chemokine CCL2 in tumors from doxycycline-induced MMTV-mS100a7a15 mice. CCL2 has been shown to recruit inflammatory monocytes/macrophages that in turn stimulate breast tumor growth and metastasis (44). In breast cancer, macrophage infiltration and CCL2 expression have been correlated with metastatic disease and poor prognosis (45–47).

We also observed significant increase in spontaneous metastasis and M2 TAMs in orthotopic syngeneic MMTV-mS100a7a15 mouse model. Previous studies have shown that TAMs promote metastasis by enhancing prometastatic and proangiogenic activities within the tumor microenvironment (17, 18, 20). We have shown enhanced expression of prometastatic and proangiogenic molecules such as CCL2 and VEGF in metastatic lung tissues. Also, we observed enhanced gene expression of *CCL2*, *VEGF*, *COX2*, and *MMP9* in primary tumors.

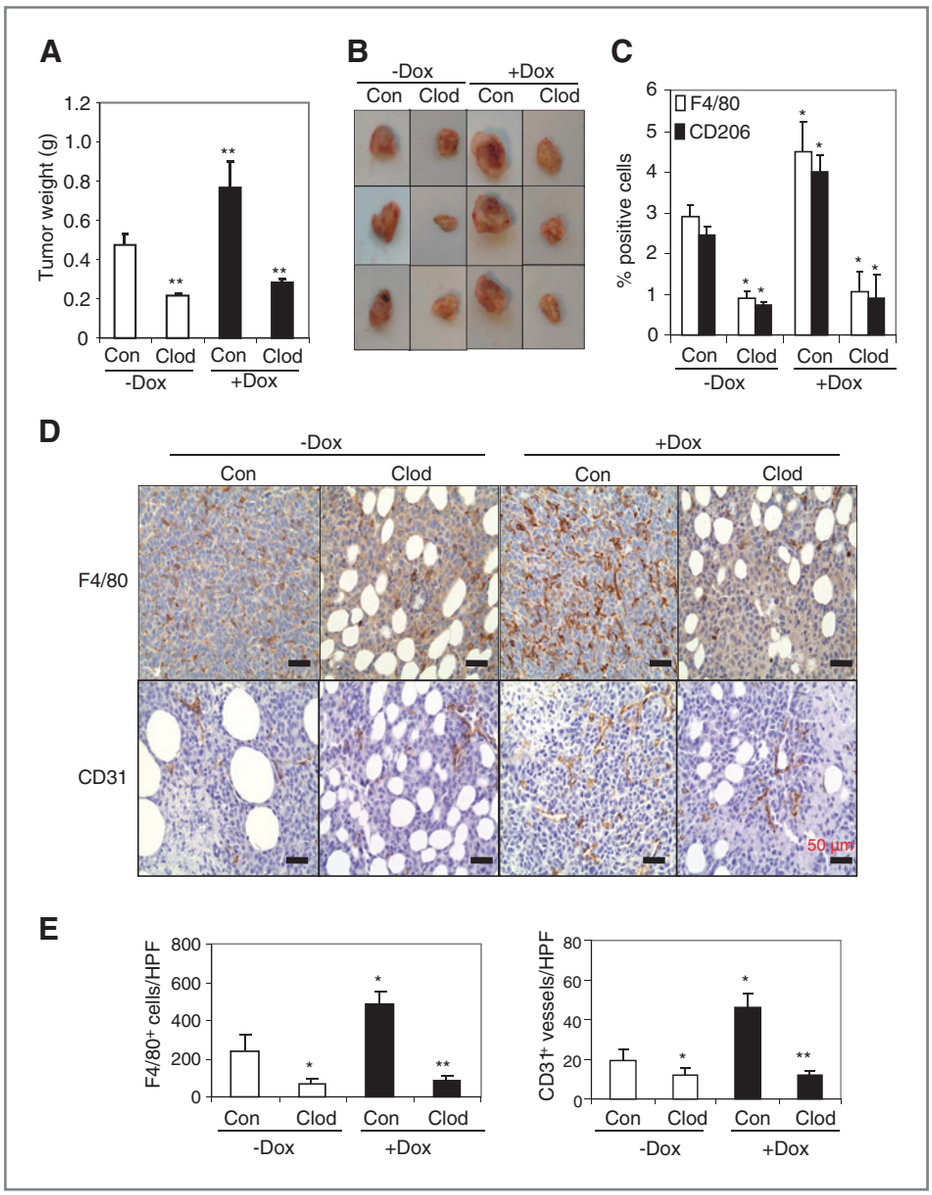


**Figure 6.** Effect of macrophage depletion on tumor growth and angiogenesis. A, growth of MVT-1–derived tumors in doxycycline-induced or uninduced MMTV-mS100a7a15 mice treated with either clodrolip (Clod) or control liposomes (Con). B, representative photograph of tumors derived from different experimental groups. C, quantitative analyses of F4/80$^+$ macrophages (white columns) or CD206$^+$ M2 macrophages (black columns) by FACS. Graphs represent the mean ± SD (control, $n = 4$; clodrolip, $n = 5$) $^*$, $P < 0.05$; $^{**}$, $P < 0.01$. D, representative immunohistochemical staining of mammary tumor sections treated with clodrolip and control liposomes with macrophage marker F4/80 antibody (top) and with endothelial marker CD31 antibody (bottom) to assess the number of macrophages infiltrating into tumors and increase angiogenesis in tumors from doxycycline-treated compared with untreated mice. E, bars represent the mean ± SD of the number of F4/80$^+$ macrophages (left) and CD31$^+$ blood vessels (right) as shown in (D) and counted in 5 random HPF (20×) per tissue section (control, $n = 4$; clodrolip, $n = 5$) $^*$, $P < 0.05$; $^{**}$, $P < 0.01$.

These molecules have been shown to enhance metastasis of various cancers (33, 44, 48–50). Previously, it has been shown that hS100A7 modulates VEGF expression in MDA-MB-468 cells (7). These studies suggest hS100A7 which has been shown to be associated with highly invasive breast cancer subtypes (31) may enhance metastasis through enhancement of pro-metastatic and angiogenic molecules.

In summary, using novel mS100a7a15 transgenic and orthotopic syngeneic mouse models, we have shown that mS100a7a15 overexpression in mammary epithelial cells enhances hyperplasia, tumor growth, angiogenesis, and metastasis. As shown in model (Supplementary Fig. S1), our studies for the first time revealed that hS100A7/mS100a7a15 produced by epithelial cells may enhance proliferation and recruit TAMs to tumor site by endocrine mechanism through RAGE activation. Recruitment of TAMs into tumor microenvironment may in turn stimulate tumor growth and metastasis by enhancing expression of prometastatic and proinflammatory molecules such as CCL2, COX2, MMP9, and VEGF. Thus, these studies suggest that S100A7 may enhance tumor growth and metastasis especially in ERα$^-$ tumors through a novel mechanism by activating proinflammatory and metastatic pathways.

## Disclosure of Potential Conflicts of Interest

No potential conflicts of interest were disclosed.

## Acknowledgments

The authors thank Susie Jones for IHC and Mohamed Adel and Zameer Gill for technical help.

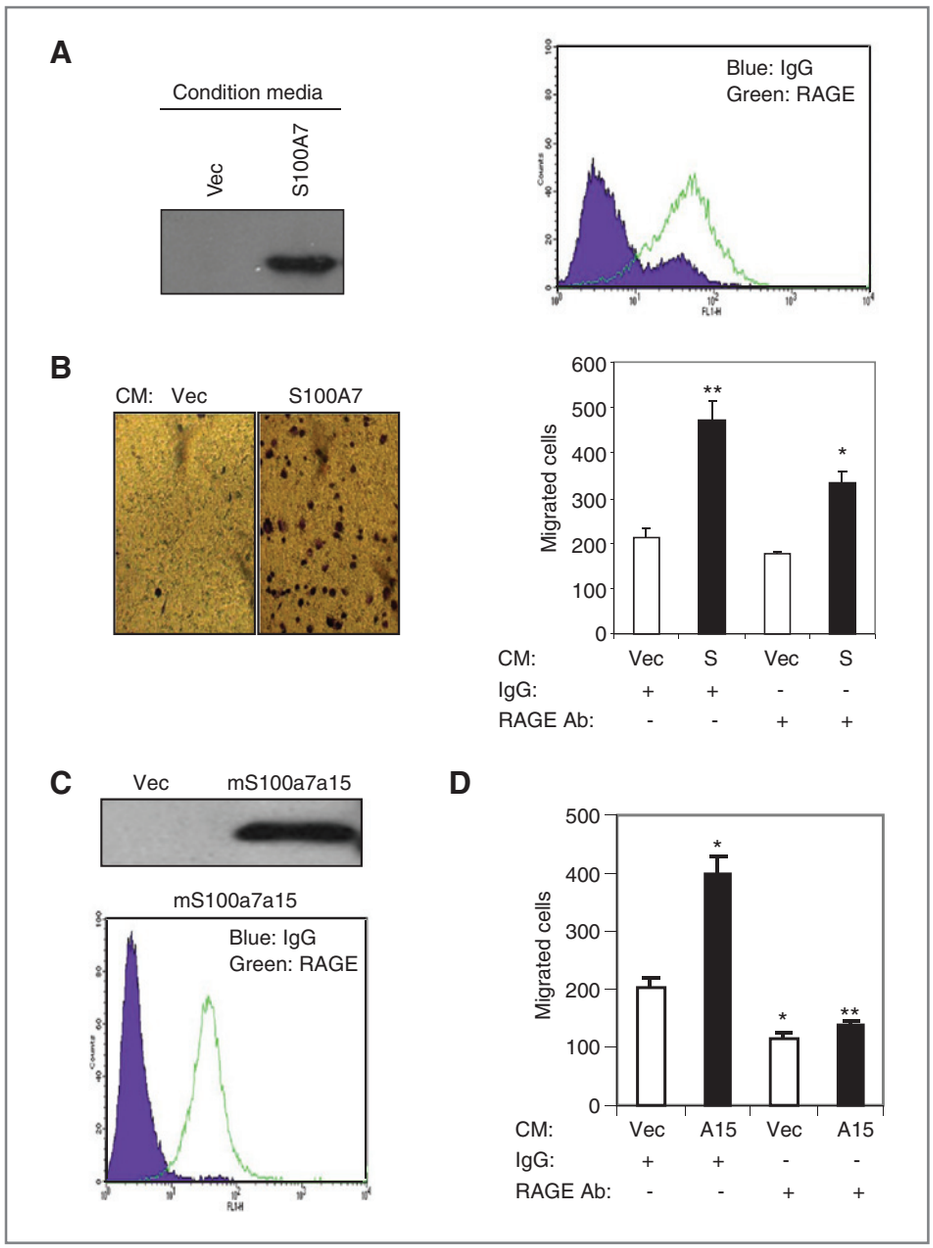


**Figure 7.** Role of RAGE in hS100A7 and mS100a7a15-induced chemotaxis of macrophages. A, Western blot of conditioned media (CM) obtained from vector (Vec) or hS100A7-overexpressing MDA-MB-231 cells. A, left, FACS analysis of RAGE expression in TDM. B, left, representative photographs of migrated TDM under phase contrast microscope. B, right, TDMs were subjected to hS100A7 or vector conditioned media–induced migration in presence of RAGE-neutralizing or control antibodies. C, top, Western blot of conditioned media of vector or mS100a7a15-overexpressing cells. C, bottom, FACS analysis of RAGE expression in MMR. D, MMR were subjected to vector or mS100a7a15 conditioned media–induced migration in presence of murine RAGE neutralizing or control antibodies. S represents hS100A7 and A15 represents mS100a7a15. Graphs represent the mean ± SD for each experiment repeated 3 times with similar results. *, $P < 0.05$; **, $P < 0.01$.

## Grant Support

This work was supported in part by grants from NIH (CA109527 and CA153490) and Department of Defense to R.K. Ganju. Y.S. Deol was supported by Pelotonia Fellowship from the Comprehensive Cancer Center, Ohio State University.

The costs of publication of this article were defrayed in part by the payment of page charges. This article must therefore be hereby marked *advertisement* in accordance with 18 U.S.C. Section 1734 solely to indicate this fact.

Received February 28, 2011; revised December 1, 2011; accepted December 3, 2011; published OnlineFirst December 12, 2011.

## References

1. Donato R. S100: a multigenic family of calcium-modulated proteins of the EF-hand type with intracellular and extracellular functional roles. Int J Biochem Cell Biol 2001;33:637–68.
2. Al-Haddad S, Zhang Z, Leygue E, Snell L, Huang A, Niu Y, et al. Psoriasin (S100A7) expression and invasive breast cancer. Am J Pathol 1999;155:2057–66.
3. Enerback C, Porter DA, Seth P, Sgroi D, Gaudet J, Weremowicz S, et al. Psoriasin expression in mammary epithelial cells *in vitro* and *in vivo*. Cancer Res 2002;62:43–7.
4. Emberley ED, Murphy LC, Watson PH. S100A7 and the progression of breast cancer. Breast Cancer Res 2004;6:153–9.

5. Emberley ED, Niu Y, Leygue E, Tomes L, Gietz RD, Murphy LC, et al. Psoriasin interacts with Jab1 and influences breast cancer progression. Cancer Res 2003;63:1954–61.
6. Emberley ED, Niu Y, Njue C, Kliewer EV, Murphy LC, Watson PH. Psoriasin (S100A7) expression is associated with poor outcome in estrogen receptor-negative invasive breast cancer. Clin Cancer Res 2003;9:2627–31.
7. Krop I, Marz A, Carlsson H, Li X, Bloushtain-Qimron N, Hu M, et al. A putative role for psoriasin in breast tumor progression. Cancer Res 2005;65:11326–34.
8. Emberley ED, Niu Y, Curtis L, Troup S, Mandal SK, Myers JN, et al. The S100A7-c-Jun activation domain binding protein 1 pathway enhances prosurvival pathways in breast cancer. Cancer Res 2005;65: 5696–702.
9. Paruchuri V, Prasad A, McHugh K, Bhat HK, Polyak K, Ganju RK. S100A7-downregulation inhibits epidermal growth factor-induced signaling in breast cancer cells and blocks osteoclast formation. PLoS One 2008;3:e1741.
10. West NR, Watson PH. S100A7 (psoriasin) is induced by the proinflammatory cytokines oncostatin-M and interleukin-6 in human breast cancer. Oncogene 2010;29:2083–92.
11. Perrier S, Caldefie-Chezet F, Vasson MP. IL-1 family in breast cancer: potential interplay with leptin and other adipocytokines. FEBS Lett 2009;583:259–65.
12. Ranger JJ, Levy DE, Shahalizadeh S, Hallett M, Muller WJ. Identification of a Stat3-dependent transcription regulatory network involved in metastatic progression. Cancer Res 2009;69:6823–30.
13. Hsieh FC, Cheng G, Lin J. Evaluation of potential Stat3-regulated genes in human breast cancer. Biochem Biophys Res Commun 2005;335:292–9.
14. Clarkson RW, Boland MP, Kritikou EA, Lee JM, Freeman TC, Tiffen PG, et al. The genes induced by signal transducer and activators of transcription (STAT)3 and STAT5 in mammary epithelial cells define the roles of these STATs in mammary development. Mol Endocrinol 2006;20:675–85.
15. Niu G, Wright KL, Huang M, Song L, Haura E, Turkson J, et al. Constitutive Stat3 activity up-regulates VEGF expression and tumor angiogenesis. Oncogene 2002;21:2000–8.
16. Allavena P, Sica A, Solinas G, Porta C, Mantovani A. The inflammatory micro-environment in tumor progression: the role of tumor-associated macrophages. Crit Rev Oncol Hematol 2008;66:1–9.
17. Sica A, Allavena P, Mantovani A. Cancer related inflammation: the macrophage connection. Cancer Lett 2008;267:204–15.
18. Pollard JW. Tumour-educated macrophages promote tumour progression and metastasis. Nat Rev Cancer 2004;4:71–8.
19. Lin EY, Nguyen AV, Russell RG, Pollard JW. Colony-stimulating factor 1 promotes progression of mammary tumors to malignancy. J Exp Med 2001;193:727–40.
20. Lin EY, Pollard JW. Tumor-associated macrophages press the angiogenic switch in breast cancer. Cancer Res 2007;67:5064–6.
21. Zeisberger SM, Odermatt B, Marty C, Zehnder-Fjallman AH, Ballmer-Hofer K, Schwendener RA. Clodronate-liposome-mediated depletion of tumour-associated macrophages: a new and highly effective antiangiogenic therapy approach. Br J Cancer 2006;95: 272–81.
22. Webb M, Emberley ED, Lizardo M, Alowami S, Qing G, Alfia'ar A, et al. Expression analysis of the mouse S100A7/psoriasin gene in skin inflammation and mammary tumorigenesis. BMC Cancer 2005;5:17.
23. Wolf R, Voscopoulos CJ, FitzGerald PC, Goldsmith P, Cataisson C, Gunsior M, et al. The mouse S100A15 ortholog parallels genomic organization, structure, gene expression, and protein-processing pattern of the human S100A7/A15 subfamily during epidermal maturation. J Invest Dermatol 2006;126:1600–8.
24. Qamri Z, Preet A, Nasser MW, Bass CE, Leone G, Barsky SH, et al. Synthetic cannabinoid receptor agonists inhibit tumor growth and metastasis of breast cancer. Mol Cancer Ther 2009;8:3117–29.
25. Pei XF, Noble MS, Davoli MA, Rosfjord E, Tilli MT, Furth PA, et al. Explant-cell culture of primary mammary tumors from MMTV-c-Myc transgenic mice. *In Vitro* Cell Dev Biol Anim 2004;40: 14–21.
26. Wolf R, Mascia F, Dharamsi A, Howard OM, Cataisson C, Bliskovski V, et al. Gene from a psoriasis susceptibility locus primes the skin for inflammation. Sci Transl Med 2010;2:61ra90.
27. Trimboli AJ, Cantemir-Stone CZ, Li F, Wallace JA, Merchant A, Creasap N, et al. Pten in stromal fibroblasts suppresses mammary epithelial tumours. Nature 2009;461:1084–91.
28. Zabuawala T, Taffany DA, Sharma SM, Merchant A, Adair B, Srinivasan R, et al. An ets2-driven transcriptional program in tumor-associated macrophages promotes tumor metastasis. Cancer Res 2010;70: 1323–33.
29. Raghuwanshi SK, Nasser MW, Chen X, Strieter RM, Richardson RM. Depletion of beta-arrestin-2 promotes tumor growth and angiogenesis in a murine model of lung cancer. J Immunol 2008; 180:5699–706.
30. Livak KJ, Schmittgen TD. Analysis of relative gene expression data using real-time quantitative PCR and the 2(-Delta Delta C(T)) Method. Methods 2001;25:402–8.
31. Wolf R, Voscopoulos C, Winston J, Dharamsi A, Goldsmith P, Gunsior M, et al. Highly homologous hS100A15 and hS100A7 proteins are distinctly expressed in normal breast tissue and breast cancer. Cancer Lett 2009;277:101–7.
32. Al-Bazz YO, Brown BL, Underwood JC, Stewart RL, Dobson PR. Immuno-analysis of phospho-Akt in primary human breast cancers. Int J Oncol 2009;35:1159–67.
33. Dechow TN, Pedranzini L, Leitch A, Leslie K, Gerald WL, Linkov I, et al. Requirement of matrix metalloproteinase-9 for the transformation of human mammary epithelial cells by Stat3-C. Proc Natl Acad Sci U S A 2004;101:10602–7.
34. Wiseman BS, Werb Z. Stromal effects on mammary gland development and breast cancer. Science 2002;296:1046–9.
35. Kang JC, Chen JS, Lee CH, Chang JJ, Shieh YS. Intratumoral macrophage counts correlate with tumor progression in colorectal cancer. J Surg Oncol 2010;102:242–8.
36. Stein M, Keshav S, Harris N, Gordon S. Interleukin 4 potently enhances murine macrophage mannose receptor activity: a marker of alternative immunologic macrophage activation. J Exp Med 1992;176:287–92.
37. Wolf R, Howard OM, Dong HF, Voscopoulos C, Boeshans K, Winston J, et al. Chemotactic activity of S100A7 (Psoriasin) is mediated by the receptor for advanced glycation end products and potentiates inflammation with highly homologous but functionally distinct S100A15. J Immunol 2008;181:1499–506.
38. Mantovani A, Schioppa T, Porta C, Allavena P, Sica A. Role of tumor-associated macrophages in tumor progression and invasion. Cancer Metastasis Rev 2006;25:315–22.
39. Nicolini A, Carpi A, Rossi G. Cytokines in breast cancer. Cytokine Growth Factor Rev 2006;17:325–37.
40. Weinstat-Saslow D, Merino MJ, Manrow RE, Lawrence JA, Bluth RF, Wittenbel KD, et al. Overexpression of cyclin D mRNA distinguishes invasive and *in situ* breast carcinomas from non-malignant lesions. Nat Med 1995;1:1257–60.
41. Condeelis J, Pollard JW. Macrophages: obligate partners for tumor cell migration, invasion, and metastasis. Cell 2006;124:263–6.
42. Riehl A, Nemeth J, Angel P, Hess J. The receptor RAGE: bridging inflammation and cancer. Cell Commun Signal 2009;7:12.
43. Taguchi A, Blood DC, del Toro G, Canet A, Lee DC, Qu W, et al. Blockade of RAGE-amphoterin signalling suppresses tumour growth and metastases. Nature 2000;405:354–60.
44. Qian BZ, Li J, Zhang H, Kitamura T, Zhang J, Campion LR, et al. CCL2 recruits inflammatory monocytes to facilitate breast-tumour metastasis. Nature 2011;475:222–5.
45. Saji H, Koike M, Yamori T, Saji S, Seiki M, Matsushima K, et al. Significant correlation of monocyte chemoattractant protein-1 expression with neovascularization and progression of breast carcinoma. Cancer 2001;92:1085–91.
46. Ueno T, Toi M, Saji H, Muta M, Bando H, Kuroi K, et al. Significance of macrophage chemoattractant protein-1 in macrophage recruitment,

angiogenesis, and survival in human breast cancer. Clin Cancer Res 2000;6:3282–9.

47. Valkovic T, Lucin K, Krstulja M, Dobi-Babic R, Jonjic N. Expression of monocyte chemotactic protein-1 in human invasive ductal breast cancer. Pathol Res Pract 1998;194:335–40.
48. McLean MH, Murray GI, Stewart KN, Norrie G, Mayer C, Hold GL, et al. The inflammatory microenvironment in colorectal neoplasia. PLoS One 2011;6:e15366.
49. Nam JS, Kang MJ, Suchar AM, Shimamura T, Kohn EA, Michalowska AM, et al. Chemokine (C-C motif) ligand 2 mediates the prometastatic effect of dysadherin in human breast cancer cells. Cancer Res 2006;66:7176–84.
50. Wang D, Wang H, Brown J, Daikoku T, Ning W, Shi Q, et al. CXCL1 induced by prostaglandin E2 promotes angiogenesis in colorectal cancer. J Exp Med 2006;203:941–51.